Naval Research Laboratory

Washington, DC 20375-5320

NRL/MR/6180--00-8489

Application of CFAST to Shipboard Fire Modeling II. Specification of Complex Geometry

J.B. HOOVER
P.A. TATEM

Navy Technology Center for Safety and Survivability
Chemistry Divison

December 29, 2000

REPORT DOCUMENTATION PAGE

Form Approved
OMB No. 0704-0188

1. AGENCY USE ONLY (*Leave Blank*)	2. REPORT DATE	3. REPORT TYPE AND DATES COVERED
	December 29, 2000	Interim Report 1998-2000

4. TITLE AND SUBTITLE

Application of CFAST to Shipboard Fire Modeling II. Specificaiton of Complex Geometry

5. FUNDING NUMBERS

6. AUTHOR(S)

J.B. Hoover and P.A. Tatem

7. PERFORMING ORGANIZATION NAME(S) AND ADDRESS(ES)

Naval Research Laboratory
Washington, DC 20375-5320

8. PERFORMING ORGANIZATION REPORT NUMBER

NRL/MR/6180--00-8489

9. SPONSORING/MONITORING AGENCY NAME(S) AND ADDRESS(ES)

Office of Naval Research
800 North Quincy Street
Arlington, VA 22217-5660

10. SPONSORING/MONITORING AGENCY REPORT NUMBER

11. SUPPLEMENTARY NOTES

12a. DISTRIBUTION/AVAILABILITY STATEMENT

Approved for public release; distribution is unlimited.

12b. DISTRIBUTION CODE

13. ABSTRACT (*Maximum 200 words*)

The use of the Consolidated Fire Growth and Smoke Transport (CFAST) fire model is well-established within the civilian community. In recent years, the U.S. Navy has sponsored enhancements to the model (including the addition of vertical vent flow, corridor flow, and improved heat conduction) to make the model more useful in Navy fire scenarios. This report is the second of a series intended to document the current state of CFAST, identify areas in need of further development work, indicate the types of Navy problems which may be addressed by CFAST, and suggest procedures for the routine application of CFAST in ship design.

14. SUBJECT TERMS

Fire modeling
CFAST
Model geometry
Shipboard fires

15. NUMBER OF PAGES

62

16. PRICE CODE

17. SECURITY CLASSIFICATION OF REPORT	18. SECURITY CLASSIFICATION OF THIS PAGE	19. SECURITY CLASSIFICATION OF ABSTRACT	20. LIMITATION OF ABSTRACT
UNCLASSIFIED	UNCLASSIFIED	UNCLASSIFIED	UL

NSN 7540-01-280-5500

Standard Form 298 (Rev. 2-89)
Prescribed by ANSI Std 239-18
298-102

CONTENTS

APPLICATION OF CFAST TO SHIPBOARD FIRE MODELING
II. SPECIFICATION OF COMPLEX GEOMETRY

1.0 INTRODUCTION

As part of an effort to increase ship survivability, the US Navy has, for several years, funded work by the National Institute of Standards and Technology (NIST) to improve the capabilities of the Consolidated Fire Growth and Smoke Transport (CFAST) model [1]. Zone fire models, of which CFAST is an example, are characterized by the use of a small number of large cells (called zones).

By definition, a zone is a homogeneous region that may be described by a single value of each state variable, such as temperature, pressure and species concentrations. Because there are few zones (CFAST, for example, uses two zones to represent an entire room) only a relatively small set of variables needs to be calculated for each time step. In addition, zone models typically use ordinary differential equations, rather than partial differential equations, to reduce the mathematical complexity of the calculations. As a result, zone models can be very fast but are limited in the amount of detail that can be provided.

A major goal of the CFAST developers was to produce a model capable of very fast execution on desktop computers. To meet this goal, certain simplifying assumptions were made regarding the types of phenomena and the complexity of the scenarios that were to be modeled. These assumptions led to limitations on the scope of the problems that can be modeled, the ease with which they can be modeled and the accuracy of the results.

The impact of these limitations on the ability of CFAST to model naval fire protection problems is not known. As a result, the Office of Naval Research has funded a project, entitled "Analysis of the CFAST Fire Model Operating Envelope," the purposes of which are to identify CFAST limitations; to determine their effects on shipboard fire modeling; and to develop methods for circumventing those problems that have significant adverse effects.

Reference [2] discussed the necessity for providing a time-dependent description of the fire and some of the problems involved in developing such a specification. It also included more detailed background information regarding CFAST, which will not be repeated here. The present work expands on the earlier report by addressing issues related to the complex geometry that is typical of ships. As in that earlier work, we have used CFAST version 3.1.4[1], except as specifically noted.

As a case study, we have again used test 4_10 from the Submarine Ventilation Doctrine [3] program. That test was conducted during January 1996 aboard the ex-USS SHADWELL in the SHADWELL/688 test area (Figure 1), which represented the forward half of a USS LOS ANGELES (SSN 688) class submarine. This particular test was selected for study because the fire compartment was a geometrically simple starting point and because the ventilation ducts were sealed. The latter factor significantly reduced the complexity of the problem, since we only had to contend with flows through hatches and doors.

In the first phase of this project, only the geometrically simple fire compartment (the Laundry Room) was modeled so that we could concentrate on the fire itself. In the present work, we expand upon that base by adding surrounding compartments while keeping the fire specification from the previous work.

---

[1] Version 4 has been under development at NIST but, as of the date of this work, had not been released for public use.

Manuscript approved November 21, 2000.

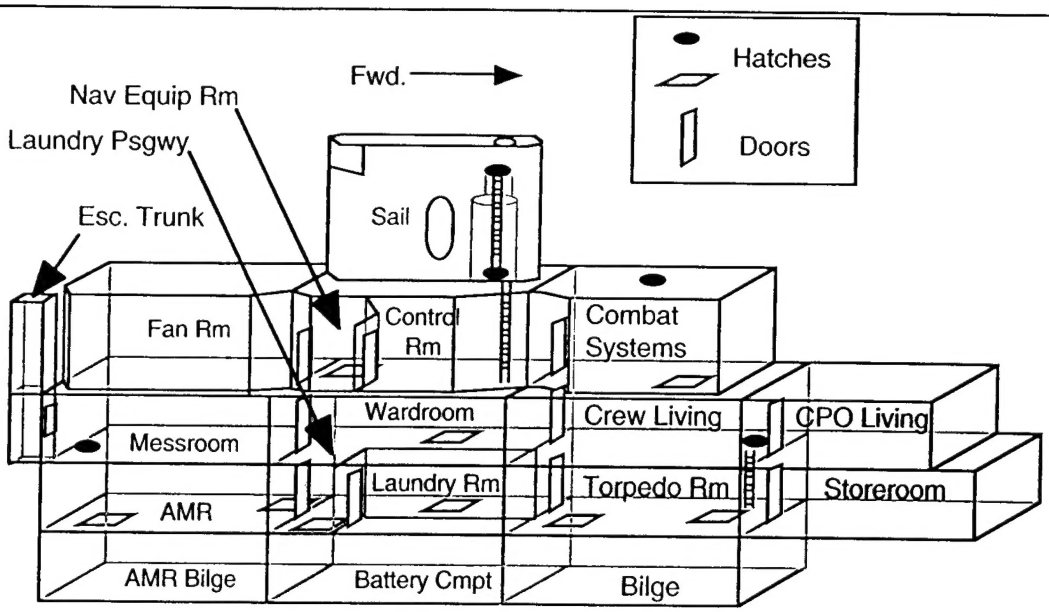

Figure 1. Test Configuration for the Submarine Ventilation Doctrine Test Program

The fires modeled during this study were diesel pan fires, located in the laundry room.

As before, we ignored most of the test data until after the modeling was completed, at which time the model predictions were compared with test results to determine the accuracy of the model. This procedure minimized the bias due to foreknowledge of the actual test outcomes.

2.0 LIMITATIONS OF CFAST GEOMETRY

Just as the vocabulary of a language limits the subjects which may be discussed in that language, so the limitations in CFAST input capabilities restrict the scenarios that can be adequately described and, of course, problems which can not be described to CFAST can not be modeled by CFAST. In this section, we discuss these limits, as they relate to the specification of the geometry for a fire simulation, present some general principles for circumventing these limitations and consider some practical problems that were encountered during our modeling effort.

2.1 Implicit Limitations of the Geometry Specification

The CFAST keywords which have been used in this model, along with brief explanations of their meanings, are presented in Appendix A. Details of the entire CFAST "vocabulary" may be found in the CFAST users' guide [4] and will not be repeated here. However, we note that the limitations of the CFAST input file format impose some restrictions on our ability to define complicated geometries, including the following:

a. compartments are limited to rectangular parallelepipeds (all compartment boundaries are rectangular);

b. each compartment has only a single bulkhead, which wraps around all four sides;

c. for any compartment, the overhead, deck and bulkheads are each limited to a single set of thermophysical properties;

d. vent locations are undefined;

e. all horizontal vents are rectangular; and

f. vertical vents must be either circular or square.

The first limitation is due to the fact that the dimensions of each compartment are described by only three parameters: DEPTH, WIDTH and HEIGH. This implies that there are exactly six bounding surfaces, each of which is a rectangle. The deck and overhead are assumed to be identical and CFAST always calculates their area as

$$A_{deck} = A_{ovhd} = \text{DEPTH} * \text{WIDTH} \qquad \text{Eqn. 1}$$

Since there is no provision for defining the individual walls, CFAST treats a compartment's vertical boundary as one continuous entity[2], with area

$$A_{blkhd} = 2 * (\text{DEPTH} + \text{WIDTH}) * \text{HEIGH} \qquad \text{Eqn. 2}$$

As a corollary, there is no way to specify in which bulkhead a horizontal vent is located. Also, each boundary has only one associated entry in the thermophysical properties database. Thus, the deck, overhead and the entire wrap-around bulkhead each has only one set of properties — it is not possible to exactly represent compartment boundaries that have patches composed of different materials[3].

Horizontal and vertical vents are defined by the keywords HVENT and VVENT, respectively[4]. HVENT has six required parameters, two of which specify the two connected compartments. CFAST permits up to four horizontal vents connecting the same pair of compartments, so the third parameter is a number that uniquely identifies each of these vents. The last three parameters are the vent width, the height of the soffit (top) and the height of the sill (bottom), respectively[5]. Thus, the vent is implicitly defined as a rectangle having dimensions

$$A_{hvent} = \text{WIDTH} * (\text{Soffit} - \text{Sill}) \qquad \text{Eqn. 3}$$

Note that there is no provision for specifying horizontal coordinates, so the vent's horizontal location is undefined.

For vertical vents, there are again two parameters to identify the connected compartments. At present, only one vertical vent is allowed between any two compartments, so there is no need for

---

[2] For each time step, CFAST implicitly divides the wall, at the calculated height of the interface, into an upper and a lower portion.

[3] It is possible to specify multiple boundaries composed of multiple layers where each layer may have different properties. For example, a bulkhead could be specified as having a steel core with cork on one side and fiberglass on the other.

[4] In CFAST terminology, a vent is any opening between compartments (or between a compartment and the outside), except for ventilation ducts, which have their own special set of keywords. Since we did not use ventilation ducts in these simulations, references to vents appearing in this report refer to doors, windows, hatches, scuttles and similar openings. Another oddity of CFAST nomenclature is that vents are described by the direction of the flow through the vent, not by the orientation of the vent itself. For example, a door is a horizontal vent, because it allows horizontal flow, although the orientation of the door is vertical.

[5] Soffit and sill heights are always specified with respect to the floor elevation (HI/F) of the first compartment.

an identifying vent number. The last two VVENT parameters are the vent area and a shape code, which specifies either a circular or a square opening — no other shapes are allowed.

2.2 Work-Arounds for the Geometry Specification Limitations

These inherent limitations force us to make approximations to describe many common shipboard situations. For example:

a. most shipboard compartments do not have simple, rectangular cross sections;

b. standard water tight doors are not rectangles; and

c. watertight hatches (except for scuttles) are usually neither square nor circular.

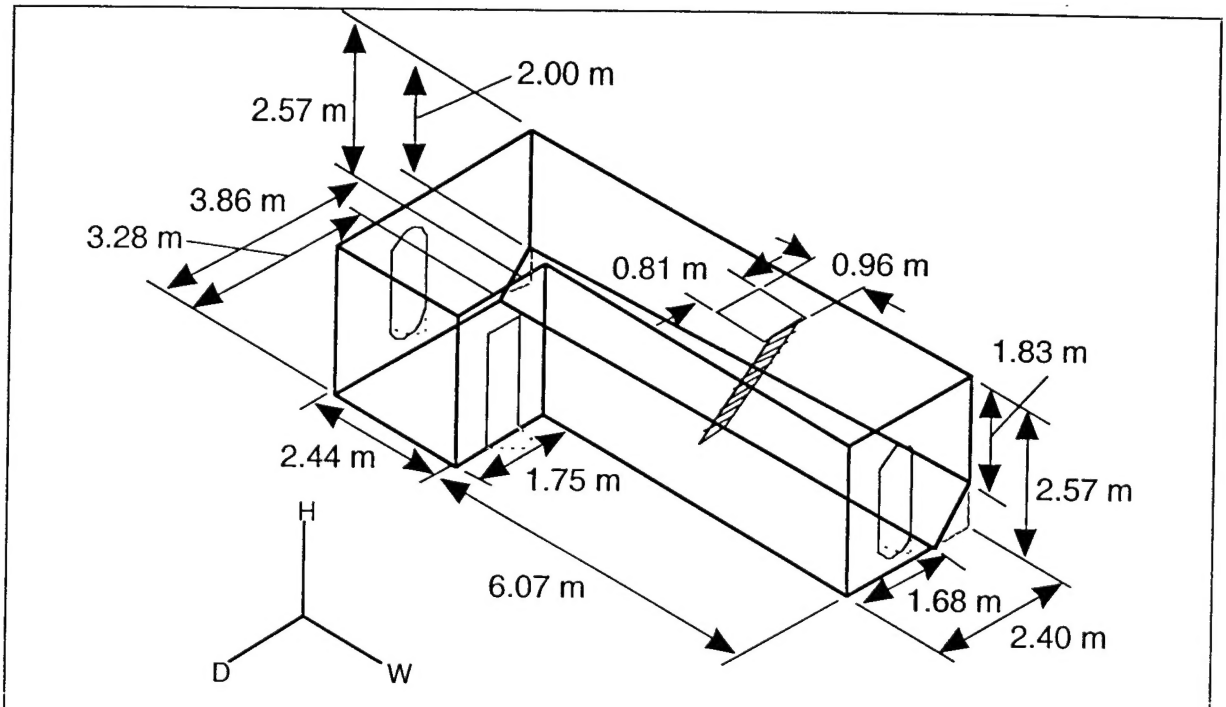

Figure 2. Laundry Passageway Dimensions

The Laundry Passageway is geometrically complex and can not be exactly represented in a CFAST input file. Several different approximation methods were tried, as discussed in the text.

The odd shapes of many shipboard compartments cause the largest problem, and the one that is usually the first to be encountered. The SHADWELL/688 Laundry Passageway (Figure 2) provides a typical example of this issue. As can be readily seen, the deck plan of this compartment is approximately L-shaped. In addition, the compartment tapers from fore to aft and the lower portion of the outboard bulkhead is cut away, producing a five-sided vertical cross section. Any one of these factors would make it impossible to create an exact description in CFAST. Somehow, this real-world complexity must be reduced to a rectangular box that is similar to the actual compartment.

2.2.1 General considerations

Before considering the specific approximations that we used, it is useful to discuss some general considerations pertinent to developing such approximations. If we consider how CFAST calculates areas and volumes, we find that Equation 1 can be used because the deck and overhead areas are constants dependent only on the input dimensions. However, CFAST can not use Equation 2 because the model operates on zones, not on entire compartments. CFAST assumes a lower layer extending from the deck to the interface height, I, and an upper layer from I to HEIGH. Since I is recalculated for each time step, the volumes of the zones are time dependent and the areas of the bulkhead regions which are in contact with each zone also vary with time. CFAST uses separate equations for the lower and upper bulkhead areas

$$A_{\text{lower blkhd}} = 2 * (\text{DEPTH} + \text{WIDTH}) * \text{I} \qquad \text{Eqn. 4a}$$

and

$$A_{\text{upper blkhd}} = 2 * (\text{DEPTH} + \text{WIDTH}) * (\text{HEIGH} - \text{I}) \qquad \text{Eqn. 4b}$$

Likewise there are two equations for the zone volumes

$$V_{\text{lower}} = \text{DEPTH} * \text{WIDTH} * \text{I} \qquad \text{Eqn. 5a}$$

and

$$V_{\text{upper}} = \text{DEPTH} * \text{WIDTH} * (\text{HEIGH} - \text{I}) \qquad \text{Eqn. 5b}$$

As long as the compartment is a rectangular parallelepiped, Equations 1, 4 and 5 are correct and self-consistent. However, a problem arises if the compartment is <u>not</u> a rectangular parallelepiped. In that case, three dimension parameters are not sufficient for an accurate description and the above equations will not be accurate. We can adjust one or more of the three inputs so that some of these equations are correct, but there is no combination of inputs that can make all of them correct. Therefore, we must decide which quantities are the most important for our simulations and attempt to ensure that those quantities are correctly calculated. The trade-off is that at least some of the remaining quantities will be incorrect and this will lead so some degree of error in the predictions.

So, how can we decide which equations to satisfy and which to sacrifice? Our approach was to start with the CFAST fire specification, which defines the fundamental energy release rate and combustion chemistry for the fire. The energy release rate and the production of combustion products are specified in terms of joules and kilograms, respectively. However, many of the interesting predictions (species concentrations, for example) are expressed in terms which involve the zone volume. Volumes enter into the calculation of mass transport between zones and even the zone temperatures can be formulated in terms of energy densities.

Mass and energy transport calculations depend on both a driving force and a resistance term. The driving force is proportional to the difference in some parameter (pressure, temperature or concentration, for example) which itself is often a function of zone volume. Resistance is typically inversely proportional to some interface area (*e.g.*, the contact area between a gas layer and the bulkhead). Therefore, the transport equations have both volume and area dependencies.

Another consideration involves horizontal vents, which may, for each of the connected compartments, be located in the lower layer, the upper layer or may span both layers. Since the layer interface is dynamic, transport through a horizontal vent can be very complex and is clearly a function of the interface height, as well as the vent parameters. Vertical vents always reside at the interface between the upper layer of one compartment and the lower layer of another and, therefore, should be independent of the interface height.

Based on the above, we expect that zone volumes will have direct effects on the initial conditions in each zone and indirect effects on mass and energy transport between zones. Since volume has direct or indirect effects on every aspect of the fire model, we considered it to be the most critical factor. Accordingly, we imposed the requirement that our approximate compartment dimensions be chosen so as to give the correct volumes.

Both surface areas and compartment heights are important for transport calculations. Unfortunately, given the constraint of a fixed volume, these are not independent parameters. If our primary interest is in horizontal fire spread and there are horizontal vents, then we will typically use the actual compartment heights to ensure that the interaction between the layer interface and the vent is handled properly. Of course, by doing this, we have implicitly fixed the overhead and deck areas as

$$A_{deck} = A_{ovhd} = \text{DEPTH} * \text{WIDTH} = V_{act} / H_{act} \qquad \text{Eqn. 6}$$

and the only remaining option is to specify either DEPTH or WIDTH, the other being determined by Equation 6.

On the other hand, if the primary goal is to simulate vertical conduction through decks, then it is important that the overhead and deck areas be accurate. In this event, a better procedure might be to conserve compartment volumes and overhead areas. The compartment height would then be

$$\text{HEIGH} = V_{act} / A_{ovhd} \qquad \text{Eqn. 7}$$

which again provides some freedom in selecting DEPTH or WIDTH.

In either case, the choice of DEPTH and WIDTH was somewhat arbitrary; typically, we used the actual value of one of these parameters, if an unambiguous value was available. Since the version of CFAST available for this project does not support horizontal heat conduction between compartments, we did not make a special effort to correctly specify bulkhead areas.

Because vents directly influence both mass and energy transport, correctly specifying the vent parameters was also important. Therefore, vent areas and shapes were chosen to be as accurate as possible. For horizontal vents, if any adjustments had to be made (as discussed below), the sill and soffit heights took precedence over the vent width because the heights had a greater impact on vent flow calculations. In our simulations, vertical vents always required some approximation since the hatches were rectangular rather than square.

2.3 Practical Limitations of CFAST

In addition to the intrinsic CFAST limitations that were discussed above, we encountered a number of practical problems in some of our simulations. The nature of the equation set that must be solved at each time step makes analytical solutions impossible so an iterative solution strategy is necessary. As a result, the progress of the model is highly dependent on the ability of the numerical solver to reach convergence. In a number of cases, we found that specific

combinations of input parameters caused the solver to either fail to converge or to require so many iterations as to be effectively useless.

Unfortunately, there does not appear to be any way to determine, *a priori*, which parameter combinations will cause a problem and which will not; nor is there any way, other than experiment, to determine what the threshold value might be when there is a convergence problem. Thus, there are scenarios which, while technically possible to model, are impossible as a practical matter.

In these instances, the only known solution is to adjust parameter values until the model runs successfully, then fine tune the parameters to be as close to reality as possible without causing CFAST to fail. For this reason, it has been found to be very advantageous to build a complex model by starting with a simple, working case and adding features, one at a time, until the desired scenario is reached.

When adding a new compartment, our approach has been to create a compartment description that is as accurate as possible, given the implicit limitations of CFAST, and then attempt to run this model. If it does not run, then we adjust some of the parameters for the new compartment until it does run. This is largely a trial-and-error process, guided by previous CFAST experience. Because feedback effects alter the results for previous compartments when a new compartment is added, we defer comparison of predictions with test data until after the entire model has been built.

Because there are feedback effects, adding a compartment often changes the overall behavior of the model as well as changing the predictions for pre-existing compartments. For these reasons, it was necessary to build the complete, multi-compartment model before meaningful comparisons with the experimental data could be made.

In addition, our procedure also provided an opportunity to revisit earlier approximations and, in some cases, to improve upon them. For example, we will discuss several instances in which the model would not run properly when the vent from the last compartment to the exterior was accurately described and, as a result, we had to substitute a smaller vent. However, we found that, after another compartment was added to the model, we were able to replace the sub-scale vent with one of the correct dimensions.

3.0 MODELING OF THE SHADWELL/688 CONFIGURATION

In keeping with the above philosophy, we began with a fire model (reported in [2]) which included only the fire compartment and a horizontal vent to the exterior. For the present work, we progressively added other compartments. For each additional compartment, we first developed one or more possible equivalent geometries based on the principles outlined above, then made empirical adjustments as necessary to get the model to run satisfactorily.

Once the model was successfully executed, the model predictions were compared with the SHADWELL/688 test results in order to estimate the accuracy of the simulation. For those cases in which two or more different approximations were developed, the test results were used to determine which approximation would be carried forward.

Because there are feedback effects, the addition of a new compartment to a model will generally change the predictions for the pre-existing compartments. For this reason, we begin by presenting the results that were previously obtained for the Laundry Room. In each of the subsequent sections, as additional compartments are included in the model, changes that were made to previously modeled compartments will be discussed.

3.1 The Laundry Room

The Laundry Room model was discussed in detail in the first report of this series [2] and that information will not be repeated here. The following summary is presented as a baseline against which the results of the current work may be compared.

3.1.1 Characteristics of the Laundry Room

As seen in Figure 3, the Laundry Room was a simple rectangular box with a single door that connected it to the rest of the ship. For this initial model, the Laundry Room was treated as if it were isolated — that is, everything outside of the door was considered to be the ambient environment. The flow restrictions of the actual ship will obviously affect the behavior of the fire and those effects were not taken into account in this simple model.

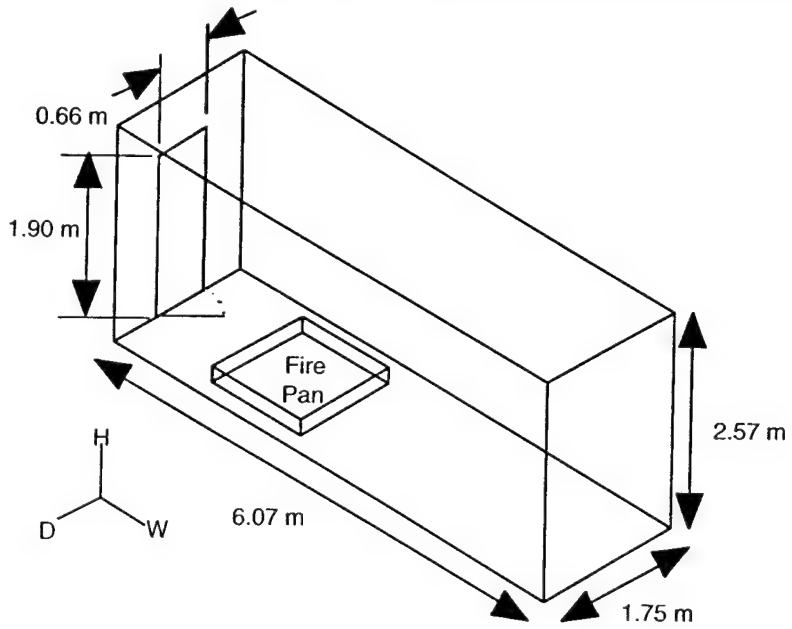

Figure 3. Laundry Room Configuration

In the test case selected for this work, the fire was located in the Laundry Room, with the fire pan centered at 0.91 (D) x 1.83 (W) x 0.19 (H). The origin of the coordinate system is the lower, left, rear corner of the compartment. Due to its geometric simplicity, this was the easiest compartment to model.

The primary purpose of the Laundry Room model was to develop an accurate description of the fire itself. That specification was based, as much as possible, on known parameters of the fuel (such as heat of combustion) and on reasonable estimates for the combustion properties (the soot production rate, for example).

3.1.2 Results of Laundry Room modeling

Temperature and gaseous species concentrations (primarily oxygen, carbon dioxide, carbon monoxide and acid gases) are the major factors in determining the habitability of a space. In the

SHADWELL/688 tests, the amount of temperature data far exceeded that for species concentration and, for some compartments, there was no species data at all. Therefore, for comparison with the tests, we focused on the CFAST temperature predictions.

In order to make these comparisons, we first had to determine, for each thermocouple, whether it corresponded to the upper or the lower layer of the model. This decision is based on the height of the interface between the layers and, as discussed in reference [2], there are two methods for estimating the interface height: calculating a value based on experimental temperature measurements[6] or relying on the model predictions. Figure 4 illustrates both methods for the case of the Laundry Room.

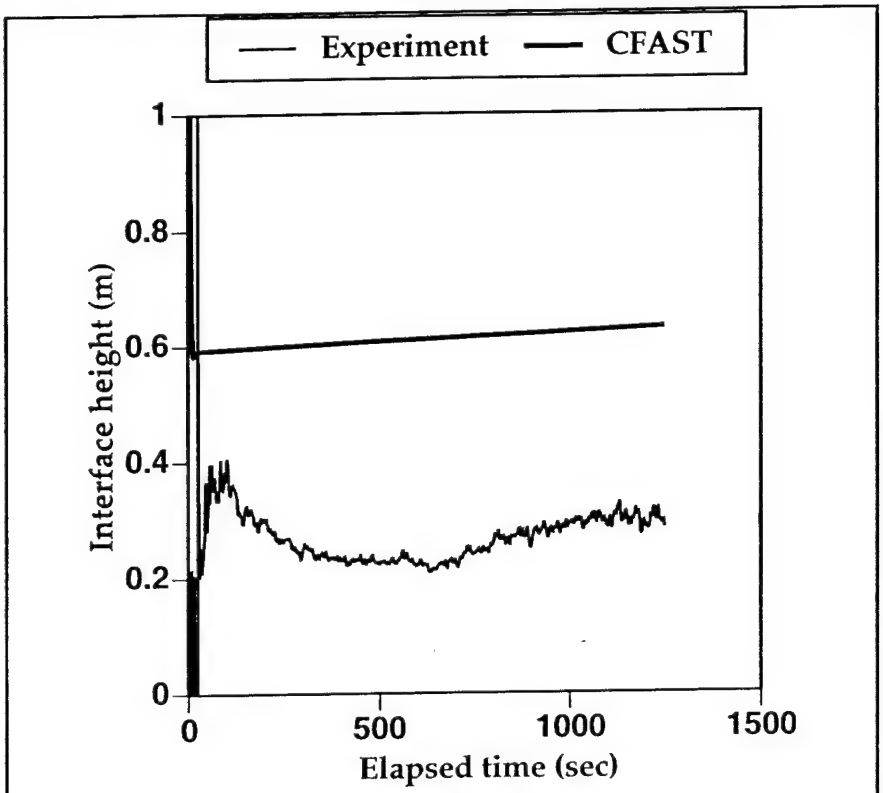

Figure 4. Laundry Room Interface Height

The height of the interface between the upper and lower layers in the Laundry Room was calculated from experimental temperature data and also by the CFAST model.

We found that the agreement between prediction and test was better when we used the CFAST-predicted interface height as the demarcation between layers. In addition, most CFAST users will not have access to test data and will have no choice in this matter. Accordingly, we have chosen to always use the model prediction when deciding in which zone a sensor lies. For simplicity, we have ignored the brief period at the beginning of the test before a quasi-steady state was reached.

[6] The method used for this calculation is presented as Equation 21 of reference [2].

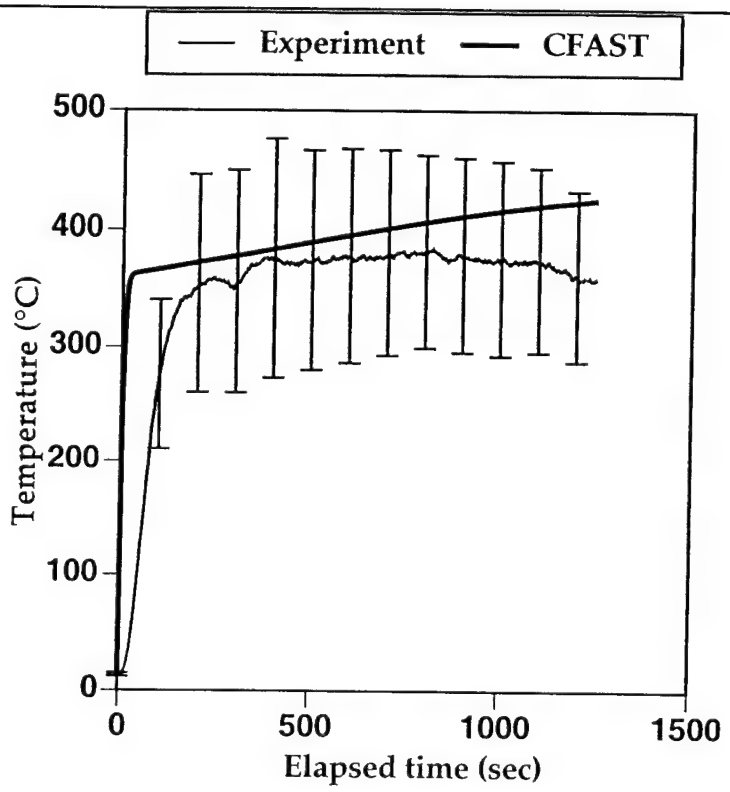

Figure 5. Comparison of Actual and Predicted Upper Layer Temperatures for the Laundry Room

For the case in which only the Laundry Room was modeled, the agreement between CFAST predictions and SHADWELL/688 test results was excellent. The error bars represent one standard deviation in the test data.

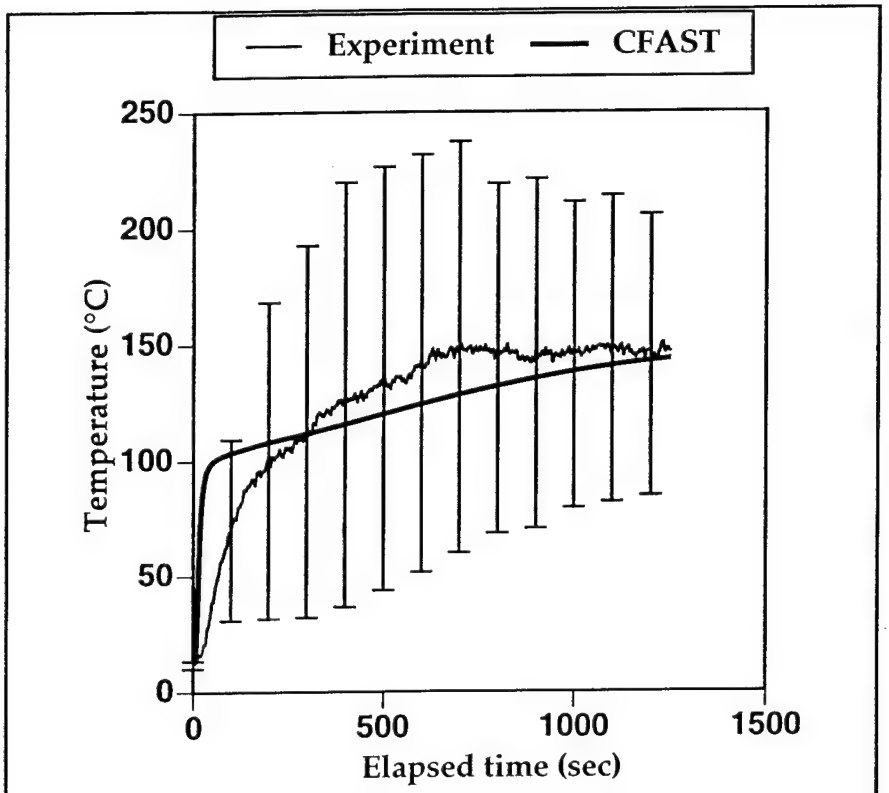

Figure 6. Comparison of Actual and Predicted Lower Layer Temperatures for the Laundry Room

Excellent agreement was also obtained for the lower layer in the Laundry Room model. The error bars represent one standard deviation in the test data.

In spite of the simplifications we made in this Laundry Room model, the temperature predictions were generally very good. As may be seen in Figures 5 and 6, the gas layer temperature predictions were in excellent agreement with the SHADWELL/688 measurements for both layers of the Laundry Room. As we will see, these Laundry Room predictions will be altered by the inclusion of additional compartments in the model.

3.2 The Laundry Passageway

The first step toward adding the Laundry Passageway was to determine, as accurately as possible, the actual volumes and surface areas of the passageway. Due to the complexity of the Laundry Passageway, this process was somewhat complicated. However, once the target values were known, the dimensions for our passageway-equivalent were easily calculated as described in the preceding example.

3.2.1 Characteristics of the Laundry Passageway

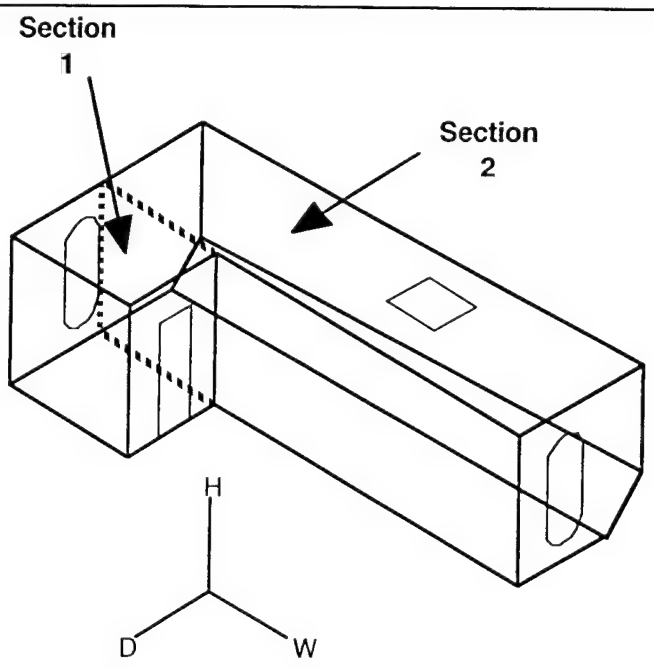

Figure 7. Conceptual Division of the Laundry Room Passageway into Sections

The dividing surface between the two sections is an aftward extension of the port bulkhead of the Laundry Room. Section 1 is then a simple rectangular region that is easy to describe. The complexity is confined to Section 2, which has an undercut along one side and tapers from fore to aft.

We first divided the compartment into two parts, Section 1 and Section 2, as illustrated in Figure 7, so that

$$V = V_1 + V_2 \qquad \text{Eqn. 8}$$

where V is the total Laundry Passageway volume and V_1 and V_2 are the volumes of Section 1 and Section 2, respectively. We note that, except for a narrow strip along one edge of Section 2, the heights of the two sections are the same, so we use

$$H_2 = H_1 = 2.57 \text{ m} \qquad \text{Eqn. 9}$$

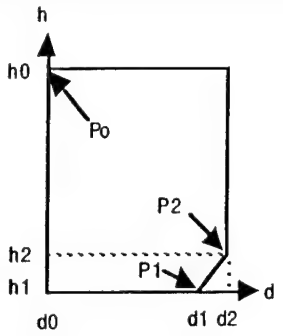

Figure 8. Cross-Section of Laundry Passageway Section 2

The cross-section of Section 2 of the Laundry Passageway (in the DH-plane) is defined by three points, P_i, having coordinates (d_i, h_i). Note that, in general, these points are functions of the w (perpendicular) coordinate.

For Section 1, the width and depth may be read directly from Figure 2

$$W_1 = 2.44 \text{ m} \qquad \text{Eqn. 10}$$

$$D_1 = 1.75 \text{ m} \qquad \text{Eqn. 11}$$

giving a volume of

$$V_1 = 10.97 \text{ m}^3 \qquad \text{Eqn. 12}$$

To calculate the volume of Section 2, consider the cross-section (in the HD-plane) shown in Figure 8. The coordinates of three points, P_0, P_1, and P_2, are sufficient to define this figure and these coordinates are functions of w, which specifies the location of the cross-section along the out-of-plane (W) axis.

From Figure 9, the top and front projections of the Laundry Passageway, we see that the coordinate functions are approximately linear in w, so we define the coordinates as follows:

$$P_0(w) = \{h_0(w), d_0(w)\} = \{H, 0\} \qquad \text{Eqn. 13a}$$

$$P_1(w) = \{h_1(w), d_1(w)\} = \{0, (m_{d1} * w + b_{d1})\} \qquad \text{Eqn. 13b}$$

$$P_2(w) = \{h_2(w), d_2(w)\} = \{(m_{h2} * w + b_{h2}), (m_{d2} * w + b_{d2})\} \qquad \text{Eqn. 13c}$$

where the various slope and intercept parameters may be determined from the dimensions given in Figure 2.

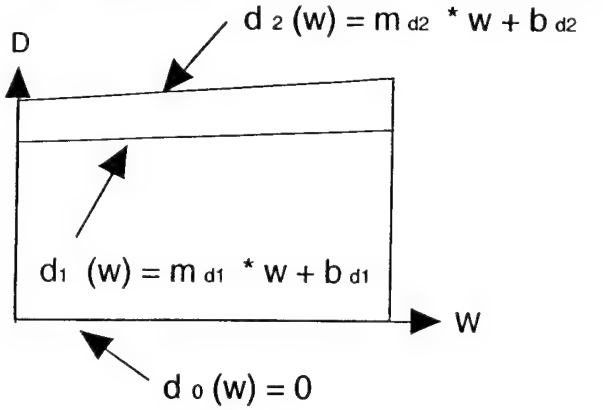

(A)

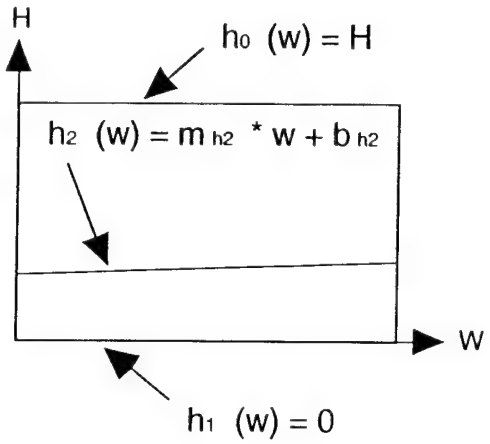

(B)

Figure 9. Top (A) and Front (B) Views of Laundry Passageway Section 2

The depth and height coordinates, d_i, and h_i, of the points that define the Laundry Passageway cross section are approximately linear functions of the width coordinate, w.

The area of the cross-section shown in Figure 8 is the area of a rectangle less the area of the cut-out triangle and, as a function of w, is given by

$$A(w) = h_0(w) * d_2(w) - [h_2(w) * (d_2(w) - d_1(w))] / 2 \qquad \text{Eqn. 14}$$

The actual volume of Section 2 is then found by integrating this cross-section over the width of Section 2

$$V_2 = \int A(w)\, dw \qquad \text{Eqn. 15}$$

Expanding the expression A(w) and integrating over the range $0 \leq w \leq W_2$, we obtain

$$V_2 = [H * m_{d2} * (W_2)^2] / 2 + H * b_{d2} * W_2 - [m_{h2} * (m_{d2} - m_{d1}) * (W_2)^3] / 6 - [b_{h2} * (m_{d2} - m_{d1}) * (W_2)^2] / 4 - [m_{h2} * (b_{d2} - b_{d1}) * (W_2)^2] / 4 - [b_{h2} * (b_{d2} - b_{d1}) * W_2] / 2 \quad \text{Eqn. 16}$$

The width of Section 2 is

$$W_2 = 8.51 \text{ m} \quad \text{Eqn. 17}$$

and, evaluating Equation 16, we get

$$V_2 = 47.50 \text{ m}^3 \quad \text{Eqn. 18}$$

From Equations 13, 21 and 22,

$$D_2 = V_2 / (H * W_2) = 2.17 \text{ m} \quad \text{Eqn. 19}$$

Quantity (units)	Psgwy (Sec 1)	Psgwy (Sec 2)
H (m)	2.57	2.57
W (m)	2.44	8.51
D (m)	1.75	2.17
V (m^3)	10.97	47.50

Table 1. Dimensions of Laundry Passageway Sections

Table 1 summarizes the dimensions that were used in the model for both sections of the Laundry Passageway. Table 2 shows the surface areas of the passageway deck, overhead and bulkheads.

Surface	Section 1		Section 2	
	Area (m^2)	Thick (cm)	Area (m^2)	Thick (cm)
A_{deck}	4.27	0.952	13.66	0.952
A_{ovhd}	4.27	0.952	19.19	0.952
A_{fwd}	4.50	0.318	5.90	0.952
A_{aft}	4.50	0.952	5.26	0.952
A_{stbd}	6.27	1.270	15.60	0.318
$A_{port,upper}$	--	--	6.30	1.905
$A_{port,lower}$	--	--	10.00	1.588
$A_{port,slant}$	--	--	7.84	1.588

Table 2. Laundry Passageway Boundary Areas and Thicknesses

Section 1 has no port bulkhead and the Section 2 port bulkhead is composed of three parts. For the overall compartment, only the total bulkhead area is meaningful.

For Section 2, the areas of the forward and aft bulkheads were calculated with Equation 14, using the appropriate values for w. The slanted portion of the port bulkhead area was treated as a trapezoid having two parallel edges the lengths of which were the hypotenuses of the dotted

triangles shown in Figure 2. The vertical part of this bulkhead was also a trapezoid, but had to be split into two parts because the hull material changed at the 1.83 m level.

The deck and overhead were made of the same 0.95 cm (0.375 in.) steel as in the Laundry Room itself. In our previous work [2], this material was defined as SHIP3/8. Because the passageway bulkheads were made of several different thickness of steel, the area-weighted mean of the various thicknesses [1.05 cm (0.414 in.)] was used, just as was done for the Laundry Room. For reference, Table 2 lists the thicknesses that were used in the model for each part of each surface. The thermal properties database entry for this material was labeled SHIPLRP.

Of the three horizontal vents in the Laundry Passageway, one has already been described as part of the Laundry Room fire specification. The other two are standard Navy water tight hatches which are 0.66 m wide, have a 0.23 m sill and a 2.04 m soffit. Unlike the Laundry Room door, these hatches have rounded corners, but the radius of curvature is relatively small (on the order of a few centimeters) and has been ignored. All three of these vents were fully opened during the tests, so each of the fractional openings (defined by the CVENT parameters) were set to 1.0.

The vertical vent is rectangular, with dimensions of 0.96 m by 0.81 m. We defined it to be a square, which is reasonably close to it actual shape, and having a vent area to (0.78 m^2) equal to that of the actual hatch.

Two alternative approaches to modeling the effects of a Laundry Room fire on the combined Laundry Room and Laundry Passageway were developed and tested. For each case, we first describe our initial CFAST inputs, including the tradeoffs and the rationales for our choices, and then consider the problems that were encountered and any modifications that had to be made to the model.

3.2.2 The two-compartment approach

Since the scenario actually involves two compartments, we used two compartments in our first model. The description of the Laundry Room itself was unchanged from our previous work [2]. For the Laundry Passageway, our goal was to create a set of effective dimensions (H_{eff}, W_{eff} and D_{eff}) which reasonably approximate the compartment shown in Figure 2.

First, we set the effective volume (*i.e.*, the volume as calculated by CFAST) to be the actual compartment volume, as calculated from Equation 8 using values from Table 1

$$V_{eff} = 58.47 \text{ m}^3 \qquad \text{Eqn. 20}$$

Since both sections had the same height, that was used as the effective height

$$H_{eff} = 2.57 \text{ m} \qquad \text{Eqn. 21}$$

In order to select values for the effective depth and width, we conceptually reassembled Sections 1 and 2 to create an equivalent geometry. Since CFAST has no knowledge of the actual orientation or position of one compartment relative to another[7], we are free to choose any configuration that is convenient. For our purposes, we chose the arrangement shown in Figure10. Essentially, we have rotated Section 2 by 90 degrees and attached it to Section 1 so that the width and depth dimensions are swapped. The effective depth of the equivalent compartment is then

[7] The one exception to this is that, by using the HI/F keyword, it is possible to specify the relative positions of the floors of different compartments.

the actual depth of Section 1 plus the actual width of Section 2. Using values from Table 1 again, we obtain

$$D_{eff} = D_1 + W_2 = 10.26 \text{ m} \qquad \text{Eqn. 22}$$

and the effective width is

$$W_{eff} = V_{eff} / (H_{eff} * D_{eff}) = 2.22 \text{ m} \qquad \text{Eqn. 23}$$

Combining these dimensions with the information regarding the construction materials and vents from the previous section, we developed the two-compartment geometry given in Listing 1[8].

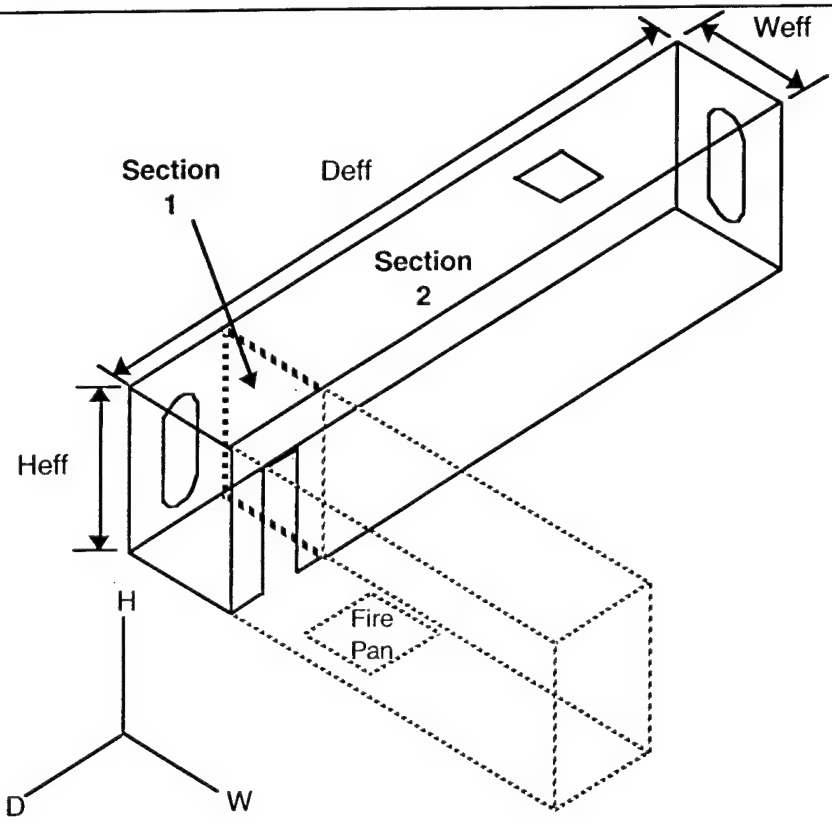

Figure 10. Equivalent Geometry of the Laundry Passageway for the Two-Compartment Model

This equivalent geometry was created by simplifying Section 2 to eliminate the undercut and the taper and then reassembling the sections. The location of the fire compartment (Laundry Room) is shown as a dotted outline for reference.

[8] Note that all lines beginning with the pound sign (#) are comments, which are ignored by CFAST.

```
#Cmpt base elevations
HI/F      0.00              0.00

#Cmpt dimensions
DEPTH     1.75             10.26
WIDTH     6.07              2.22
HEIGH     2.57              2.57

#Cmpt materials
CEILI     SHIP3/8           SHIP3/8
WALLS     SHIPLR            SHIPLRP
FLOOR     SHIP3/8           SHIP3/8

#Laundry-Passageway door
HVENT     1   2   1     0.66    1.90    0.00    0.00
CVENT     1   2   1     1.00    1.00

#Passageway-AMR door
HVENT     2   3   1     0.66    2.04    0.23    0.00
CVENT     2   3   1     1.00    1.00

#Passageway-Torpedo Rm door
HVENT     2   3   2     0.66    2.04    0.23    0.00
CVENT     2   3   2     1.00    1.00

#Passageway-Wardroom hatch
VVENT     2   3   0.78 2
```

Listing 1. File for the Two-Compartment Representation of the Laundry/Laundry Passageway Scenario

This portion of a CFAST-compatible input file represents the Laundry Room/Laundry Passageway two-compartment approximation discussed in the text. The reference elevation was chosen to be the actual deck elevation, therefore the floor height (HI/F) values for both compartments are zero. For all vent keywords, the first two parameters are the source and destination compartment numbers (1 = Laundry Rm.; 2 = Laundry Passageway; 3 = ambient environment).

3.2.3 The three-compartment approach

As mentioned above, the current version of CFAST does not make use of any information regarding the actual spatial relationships among compartments. However, for version 4.0, NIST is developing an algorithm to predict compartment-to-compartment horizontal heat transfer through bulkheads. In order for this feature to work, it will be necessary to specify the relative horizontal positions of the compartments. Thus, it makes sense to investigate modeling approaches that allow this information to be correctly specified for all compartments.

To address this issue, we have applied a method, known as virtual compartments, in which each of the Laundry Passageway sections is treated as if it were a separate compartment, giving a total of three compartments for the entire modeling domain. This approach provides more degrees of

freedom, since each section has its own dimensions and vent definitions, and thereby allows the actual relationships among compartments to be more accurately represented.

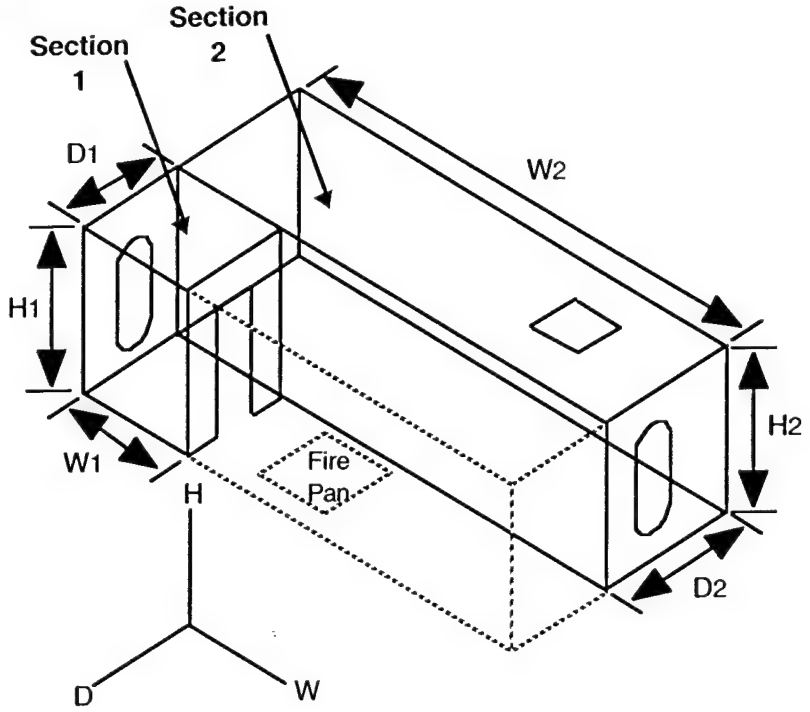

Figure 11. Equivalent Geometry of the Laundry Passageway for the Three-Compartment Model

By treating the Laundry Passageway section as if it were a separate compartment, it was possible to create a geometry that more closely resembled the actual situation. The location of the fire compartment (Laundry Room) is shown as a dotted outline for reference.

For this approach, we used the dimensions from Table 1 to define the two compartments which, taken together, represent the passageway. Compartment two is 2.44 m (W) x 1.75 m (D) x 2.57 m (H) while compartment 3 is 8.51 m x 2.17 m x 2.57 m. The ambient environment then became compartment four. The existing vents were renumbered accordingly and a new horizontal vent was defined to represent the entire 2.44 m (W) x 2.57 m (H) bulkhead between the two sections. The equivalent geometry of this layout is shown in Figure 11.

The area-weighted bulkhead thicknesses were recalculated, using the values from Table 2, to be 0.0090 cm (0.353 in.) and 0.0110 cm (0.433 in.) for compartments two and three, respectively. Two new entries, SHIPLRP1 and SHIPLRP2, were defined in the Thermal.df file to represent these materials.

The model geometry for the virtual compartment approach is shown in Listing 2.

3.2.4 The vertical vent problem

Surface	Section 1		Section 2	
	Area (m^2)	Thick (cm)	Area (m^2)	Thick (cm)
A_{deck}	4.27	0.952	13.66	0.952
A_{ovhd}	4.27	0.952	19.19	0.952
A_{fwd}	4.50	0.318	5.90	0.952
A_{aft}	4.50	0.952	5.26	0.952
A_{stbd}	6.27	1.270	15.60	0.318
$A_{port,upper}$	--	--	6.30	1.905
$A_{port,lower}$	--	--	10.00	1.588
$A_{port,slant}$	--	--	7.84	1.588

Table 2. Laundry Passageway Boundary Areas and Thicknesses

Section 1 has no port bulkhead and the Section 2 port bulkhead is composed of three parts. For the overall compartment, only the total bulkhead area is meaningful.

Unfortunately, neither of these methods was fully successful. In both cases, when the input values discussed above were used, we found that the model would not run to the end of the 1250 second simulation. For the two-compartment case, it ran at normal speeds for the first 148 seconds of the simulation (at a rate of about four simulated seconds per second of computer time[9]) but then the execution speed dropped four orders of magnitude (to approximately 3 simulated milliseconds per second). In the three-compartment model, CFAST stalled after only 78 seconds of simulation. At those rates, the model is effectively unusable because, on typical desktop computers, it would take days to complete each simulation.

This problem is due to the way in which CFAST handles the size of the time step used by the numerical solver. The step size is adjusted, upward or downward, based on the results of previous steps. The step size is increased when convergence is reached very quickly and decreased if convergence fails. Typically, the step size is on the order of milliseconds (it can be as much as several seconds when conditions are especially favorable) but, after repeated convergence failures, the step size can be reduced to a fraction of a microsecond. Under normal circumstances, simulating one second requires only hundreds or thousands of iterations but this can grow to tens of millions of iterations under adverse conditions.

In our previous experiences with models that lacked vertical vents, we seldom encountered such stalls. Therefore, suspicion immediately focused on the vertical vent in the Laundry Passageway. When this vent was removed from the input, the stall was eliminated. We then tried using vertical vents of various sizes to determine whether the problem was due to the existence of the vent or was related to the size of the vent. We expected the latter, since the validation of the vertical vent algorithm [5] had not revealed any fundamental flaws in the algorithm itself.

[9] Typical execution rates on current microcomputers are on the order of 10 simulated seconds per second. However, the solver is slower at the beginning of the simulation because it is making essentially random guesses. Once it has acquired a history of prior solutions, the solver predictions get better and it speeds up. Transient inputs (a step function change in burning rate, for example) normally cause a temporary slowdown until a new history can be developed. Also, CFAST requires several minutes to load and initialize. Since this disproportionately affects short simulations, we did not begin timing until after the startup delay.

```
#Cmpt base elevations
HI/F     0.00              0.00              0.00

#Cmpt dimensions
DEPTH    1.75              1.75              2.17
WIDTH    6.07              2.44              8.51
HEIGH    2.57              2.57              2.57

#Cmpt materials
CEILI    SHIP3/8           SHIP3/8           SHIP3/8
WALLS    SHIPLR            SHIPLRP1          SHIPLRP2
FLOOR    SHIP3/8           SHIP3/8           SHIP3/8

#Laundry-Passageway 1 door
HVENT    1   2   1    0.66    1.90    0.00    0.00
CVENT    1   2   1    1.00    1.00

#Passageway 1-AMR door
HVENT    2   4   1    0.66    2.04    0.23    0.00
CVENT    2   4   1    1.00    1.00

#Passageway 1-Passageway 2 door
HVENT    2   3   1    2.44    2.57    0.00    0.00
CVENT    2   3   1    1.00    1.00

#Passageway 2-Torpedo Rm door
HVENT    3   4   1    0.66    2.04    0.23    0.00
CVENT    3   4   1    1.00    1.00

#Passageway-Wardroom hatch
VVENT    3   4   0.78 2
```

Listing 2. File for the Three-Compartment Representation of the Laundry/Laundry Passageway Scenario

This portion of a CFAST-compatible input file represents the Laundry Room/Laundry Passageway three-compartment approximation discussed in the text. The reference elevation was chosen to be the actual deck elevation, therefore the floor height (HI/F) values for both compartments are zero. For all vent keywords, the first two parameters are the source and destination compartment numbers (1 = Laundry Rm.; 2 = Section 1 of the Laundry Passageway; 3 = Section 2 of the Laundry Passageway; 4 = ambient environment). The entire 2.44 m x 2.57 m bulkhead between the two sections is specified as a vent.

To investigate this, we ran a series of sensitivity tests in which the vent area was varied from zero to 0.78 m^2 (full size). For each test, the completion fraction was plotted as a function of the vent area. Completion fraction was defined as the number of simulated seconds prior to stalling divided by the total planned simulation time (1250 seconds). The results for the two-compartment case show that there is no problem for vent areas less than approximately 0.25 m^2 (Figure 12). For areas greater than that, the time before stalling was roughly inversely proportional to the vent area, at least up to the actual size of the vent.

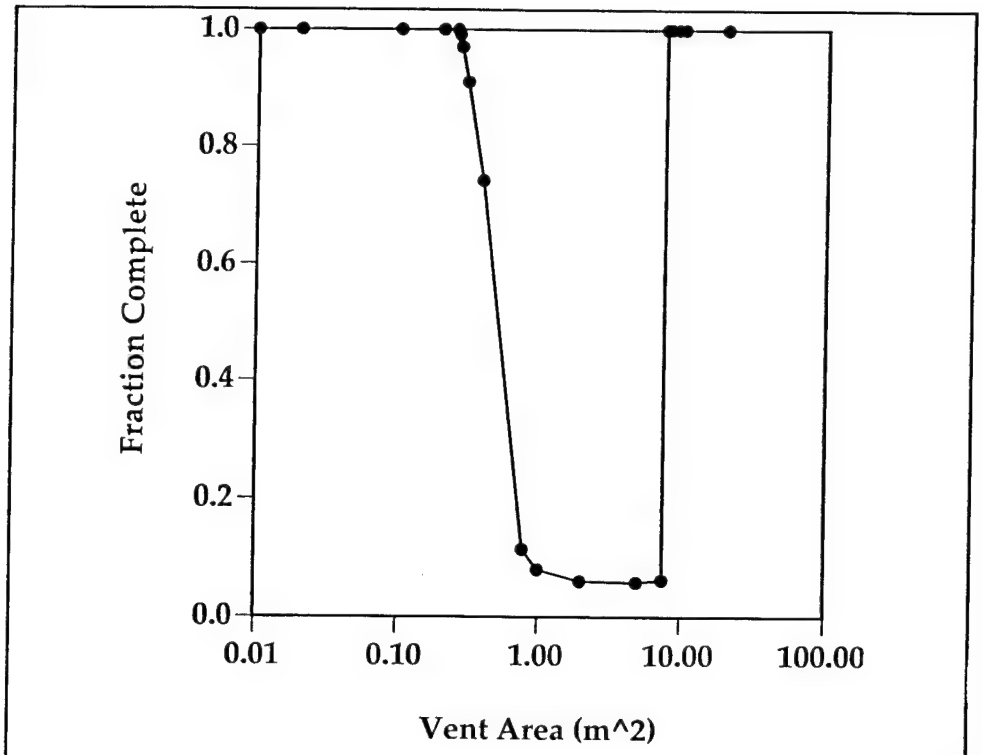

Figure 12. Completion Fraction versus Vertical Vent Area for Two-Compartment Model

The completion fraction, defined as the number of simulated seconds prior to stalling divided by the total planned simulation time, was plotted for various values of the vertical vent area (in square meters). CFAST was not able to run to completion for areas between about 0.25 m^2 and 7.5 m^2.

The situation was worse for the three-compartment model. In Figure 13, we see that stalls occurred at various times for all non-zero vent areas. Since it is obvious that model predictions for the Wardroom will not be correct if the hatch between the Laundry Passageway and the Wardroom is eliminated, we did not pursue this approach any further.

In order to decide whether the two-compartment method would be acceptable, we investigated the extent to which the vent area affects CFAST predictions. This was accomplished by conducting a sensitivity test, in which the vent area was systematically varied from zero to the actual size of the vertical vent. We then looked at the gas, wall, ceiling and floor temperature predictions for both the Laundry Room and the Laundry Passageway.

We found that, in the fire compartment (Laundry Room) itself, there was almost no detectable difference among the predictions, as might be expected. For the Laundry Passageway, the air temperatures tended to rise to a maximum in the first minutes, then abruptly drop and, finally, increase slowly for the duration of the simulation. The peak and subsequent decline are presumably due to transient effects that occur before the inter-compartment flows are fully established.

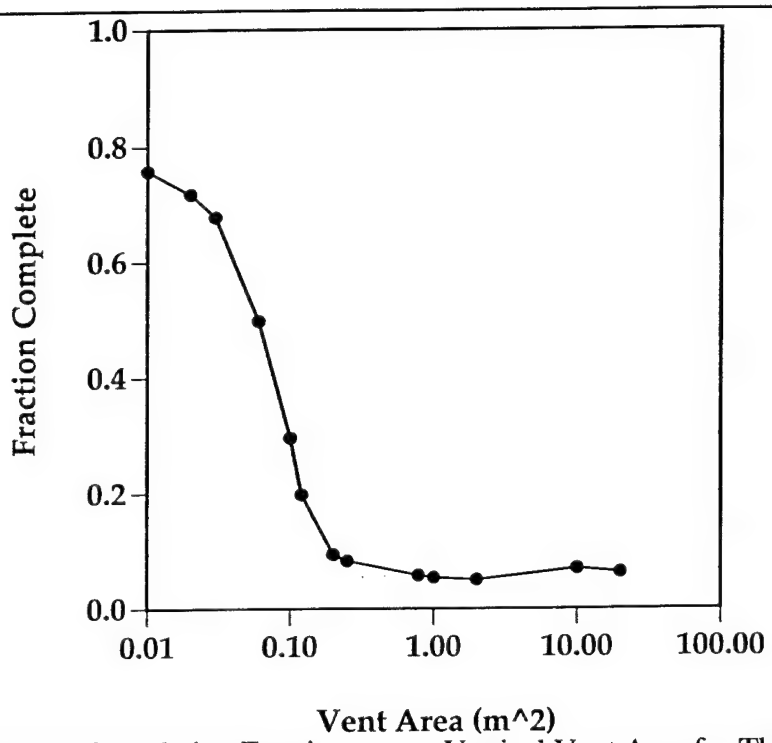

Figure 13. Completion Fraction versus Vertical Vent Area for Three-Compartment Model

For the three-compartment case, the model stalled for all non-zero vent areas.

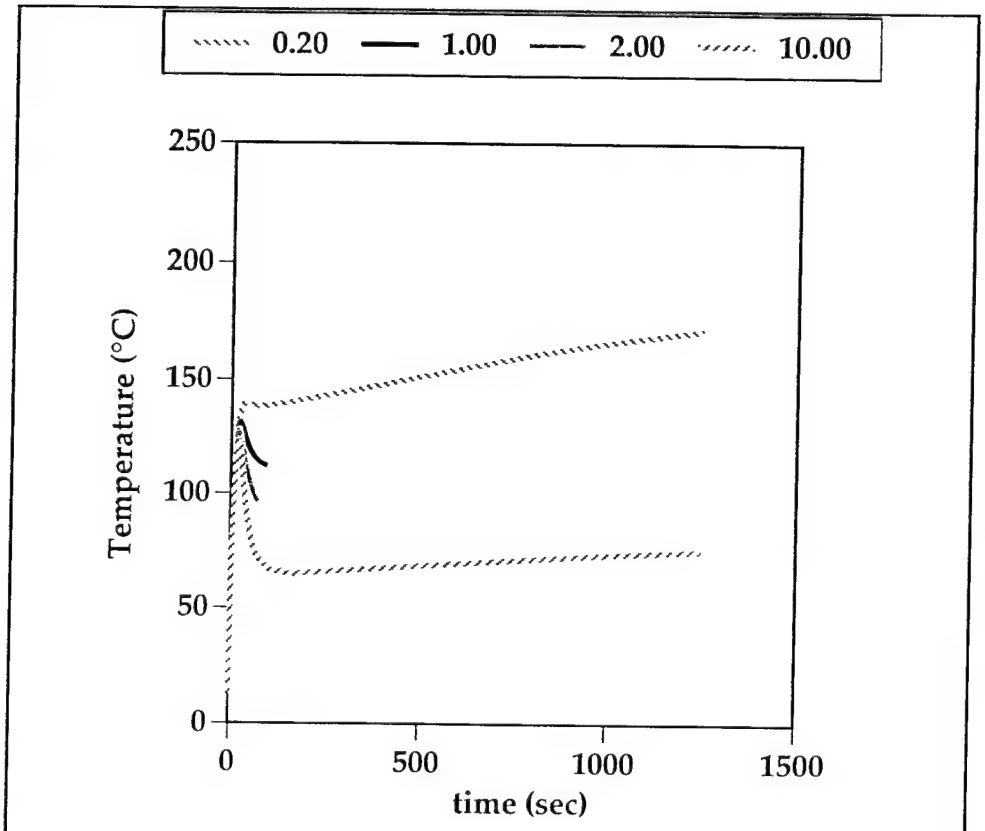

Figure 14. Upper Layer Gas Temperatures in the Laundry Passageway for Various Vent Areas

Upper layer temperatures in the Laundry Passageway decreased somewhat as the area (m^2) of the vent in the Laundry Passageway overhead was increased. This was attributed to increased venting of the hot, upper layer gas.

For the upper layer (Figure 14), the peak and quasi-equilibrium temperatures decreased as the vent area was increased. In the lower layer, the situation was more complex, as seen in Figure 15. For vents of less than a few square meters, the peak temperatures appear to increase with vent size but this maximum is significantly lower for very large vents. However, the data are inconclusive for these cases due to the stalls which occurred near or before the peak temperature was reached and which prevented quasi-equilibrium conditions from developing in many of the simulations.

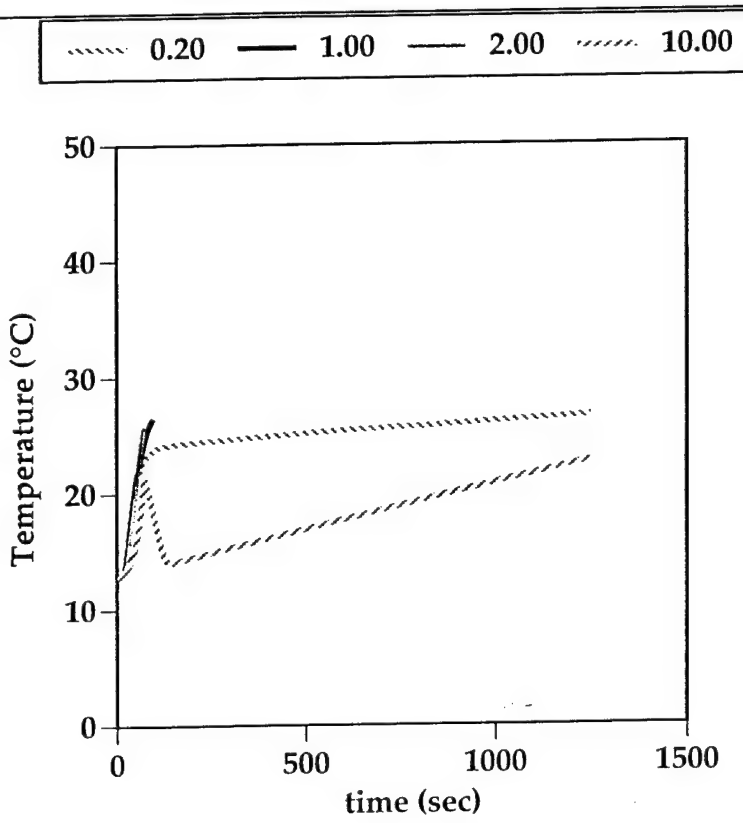

Figure 15. Lower Layer Gas Temperatures in the Laundry Passageway for Various Vent Areas

For small increases in the area (m^2) of the Laundry Passageway overhead vent, the lower layer increased slightly. This was believed to be due to increased inflow from the fire compartment. However, for very large areas, the temperature curve peaks and then drops sharply. The reasons for this behavior are not understood.

Venting of the hottest gases via an opening in the overhead would be expected to lower the air temperature, so the inverse relationship for the upper layer is in agreement with intuition. The limited data for the lower layer suggests the opposite trend — increasing temperatures with increasing vent area (except for the largest vents). A possible explanation for this behavior is that the larger vent permits increased flow into the compartment, thus bringing in larger quantities of hot gases from the adjoining fire compartment.

Based on these results, we concluded that the size of the vent does make a measurable difference in the temperature predictions for the Laundry Passageway, but that this difference is relatively

small. Therefore, it is reasonable to set the area of the vertical vent to the largest value for which CFAST does not stall during the 1250 second simulation period — 0.25 m^2, for this scenario.

3.2.5 Results of Laundry Passageway modeling

The analysis of model sensitivity to vent area was performed using nominal values for all other parameters. As was discussed in reference [2], some of the fire parameters are very dependent on the burning conditions and can vary over a wide range in real fires but, for temperature predictions, the OD (soot) parameter is the only one of these which has significant effects. Consequently, we have found it to be good practice to bracket the nominal value (0.06) of this parameter with the values zero and 0.10, which are characteristic of more extreme cases.

However, when we attempted to run the Laundry Passageway model using these extreme values, we again encountered difficulties with the model slowing to unusable execution rates. Stalls occurred at 57 and 1208 seconds for the lower and upper limiting cases, respectively. Consequently, we were forced to rely only on the predictions for the nominal case without the benefit of investigating a range of conditions.

As an aside, we note that the original stall problem was related to the vertical vent area, which suggested that the cause involved the calculation of vent flow rates. The later results indicate a connection to the soot concentration which, at first glance, appears to have little relationship with flow rates. This illustrates a general problem with complex computer models — the equations are so interdependent that changing any parameter can effect all of the other parameters and thereby cause errors in algorithms that have no direct dependence on the original parameter. In this particular case, for example, changing the OD input changes the soot concentrations and alters the radiative transport properties of the gas layers. This affects the gas temperatures that are used in the calculation of pressures and, of course, the flow rates are dependent on pressure.

3.3 The Wardroom

The Wardroom, shown in Figure 16, was one of the simpler compartments, having a trapezoidal deck and a constant height. Note that there are two vertical vents associated with the Wardroom, one in the deck and another in the overhead. The first is the Laundry Passageway vent that was previously discussed; the second is the hatch to the Navigation Equipment Room. Since the Navigation Equipment Room has not yet been added to this model, that hatch currently opens to the external environment. The two hatches are the same size and shape. Because this compartment was located directly above the Laundry and the Laundry Passageway, it was necessary to account for vertical heat conduction through the deck. Finally, there were two watertight doors in the forward bulkhead of the Wardroom. However, the starboard door led only to a void space and was always closed. We could have defined the door and set the corresponding CVENT to zero but, for simplicity, we chose not to include it in the model.

3.3.1 Characteristics of the Wardroom

Since the Wardroom tapered somewhat from fore to aft, we calculated the effective depth as the mean of the depths at the ends of the compartment. The actual compartment height and width were used. Since the various bulkheads were of different thicknesses, it was necessary to create another fictitious material, SHIPWR, using the area-weighted mean thickness approach shown in Table 3. The only complexity was due to the fact that the port and starboard bulkhead thicknesses changed at a level of 0.78 m above the Wardroom deck. Below this, the inboard and outboard bulkheads were made of 1.270 cm and 1.905 cm steel, respectively. Above the demarcation, both bulkheads were 2.222 cm thick. As a result, the equivalent bulkhead thickness was found to be 1.686 cm.

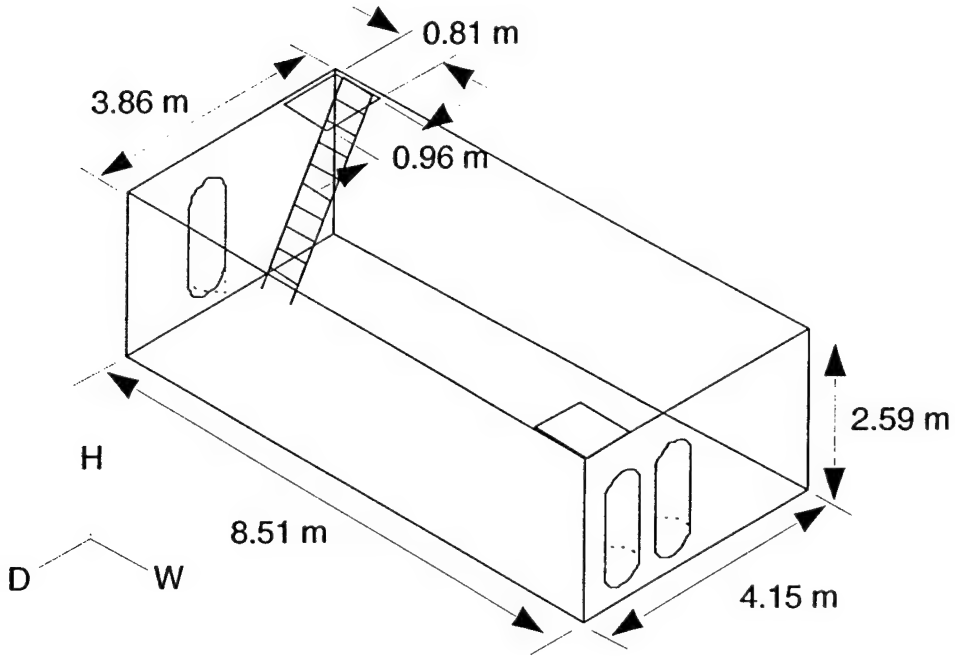

Figure 16. Wardroom Dimensions

The Wardroom is approximately a constant-height trapezoid and was relatively easy to represent.

Surface	Area (m^2)	Thick (cm)	Area*Thick (m^2-cm)
A_{fwd}	10.75	0.952	10.23
A_{aft}	10.00	0.952	9.52
$A_{port,upper}$	15.41	2.222	34.24
$A_{port,lower}$	6.64	1.905	12.65
$A_{stbd,upper}$	15.40	2.222	34.22
$A_{stbd,lower}$	6.64	1.270	8.43
Totals	64.84		109.30

Table 3. Wardroom Bulkhead Areas and Thicknesses

Due to the discontinuity in the bulkhead material 0.78 m above the deck, the port and starboard bulkheads each had to be treated as two separate parts.

Recall that, in general, CFAST has no knowledge of the geometrical relationships among the compartments. By default, the model does not know that the overhead of one compartment is the deck of another and, therefore, heat conduction between two vertically adjacent compartments is normally not calculated. However, the CFCON keyword can be used to inform CFAST that a

particular pair of compartments is vertically adjacent. When used, this keyword enables vertical heat transfer from the lower compartment to the upper[10].

3.3.2 Approaches to vertical heat conduction

Since the Wardroom overlies two compartments, the obvious approach is to connect both lower-deck compartments to the Wardroom. Unfortunately, this does not work — if two CFCON connections to the same compartment are specified, the numerical solver fails to initialize properly and causes CFAST to immediately quit. Consequently, we tried two other approaches, one in which there was heat conduction between the Wardroom and the Laundry and one in which the conduction was between the Laundry Passageway and the Wardroom.

In both cases, we found that there were stalling problems, similar to that reported above, when the correct area (0.78 m^2) of the exterior vertical vent was used. Since vertical conduction was a new phenomenon in this model, we first tried disabling that calculation to determine whether conduction was the cause of the difficulties. Without vertical conduction, the model ran correctly with the actual vent area but stalled whenever conduction was enabled for either of the lower compartments. Further experimenting revealed that the model could be made to run for either conduction configuration if the exterior vent size was reduced to 0.26 m^2 or below.

In the process, we also discovered that the addition of the Wardroom to the model lifted the restriction on the area of the hatch from the Laundry Passageway. Accordingly, we were able to change that area from 0.25 m^2 to the correct size of 0.78 m^2.

3.3.3 Results of Wardroom modeling

These results indicated that we had a choice between using the correct exterior vent area without conduction and using a sub-scale exterior vent with conduction. In the latter case, we also had to choose which pair of compartments to connect. To address these questions, we compared the effects of no conduction and conduction between two different pairs of compartments. For the latter cases, we used the largest workable exterior vent area (0.26 m^2). Simulations of the no-conduction case were run with both the correct area (0.78 m^2) and with the smaller area.

From Figure 17, we see that neither the upper nor the lower bulkhead temperatures are very sensitive to the effects of vertical conduction, with conduction from the Laundry Room having a slightly greater effect than conduction from the Laundry Passageway. For the gas temperatures (Figure 18), there are larger effects, particularly for the lower layer. Again, the greatest effect is seen when conduction is from the Laundry Room rather than from the Laundry Passageway. Finally, Figure 19 shows that conduction from the Laundry Room had a major impact on the temperature of the Wardroom deck. This is to be expected, because the fire was located in the Laundry. In the presence of conduction, the size of the external vent had no effects on the temperatures for the lower bulkhead, lower gas layer or deck in the Wardroom. Very slight reductions in the upper layer and upper bulkhead temperatures were attributed to increased venting of hot gases through the larger hatch.
Based on these findings, we chose to include the effects of conduction from the Laundry to the Wardroom, accepting that the area of the hatch from the Wardroom to the next level would have to be reduced in size, at least as a temporary expedient. Because there are feedback effects, the fact that the full-sized vent does not work when it opens into the ambient environment does not

[10] In the default case, CFAST assumes that the far side of any boundary is exposed to the external environment and therefore uses the ambient temperature for conduction calculations. Under these conditions, energy is lost from the model rather than being transferred to another compartment. CFCON changes this behavior for vertical conduction (through ceilings/floors) but does not affect horizontal heat conduction (through walls).

mean that it will not work when the next compartment, the Navigation Equipment Room, is added to the model.

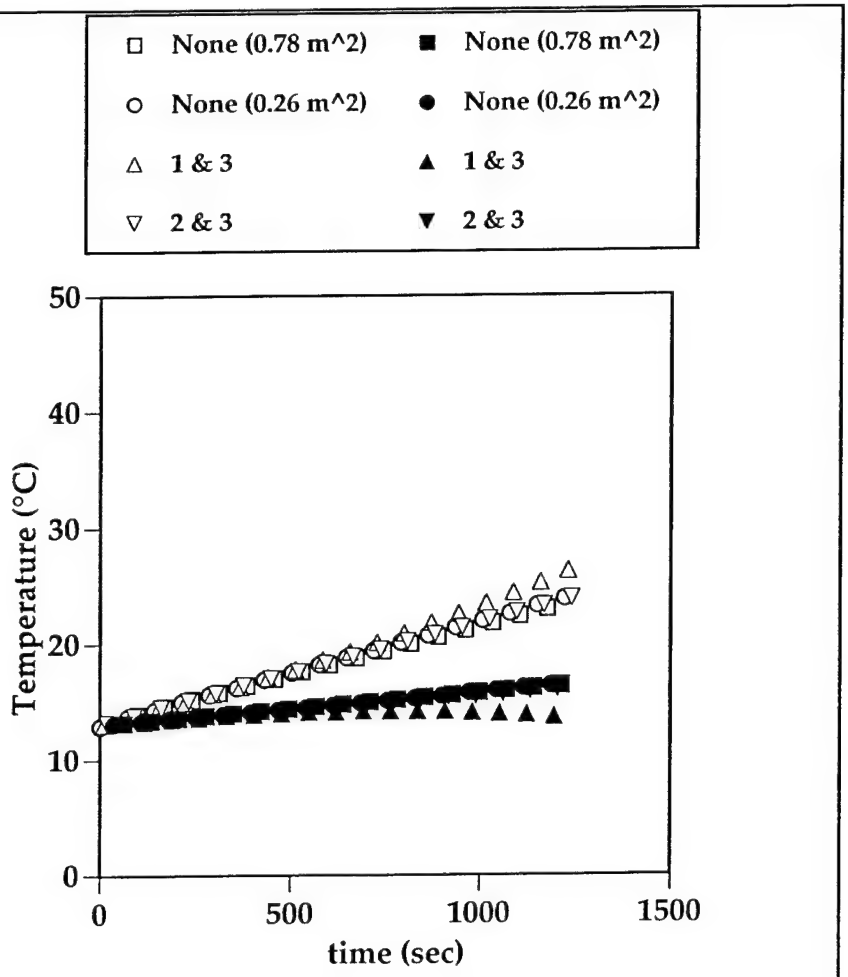

Figure 17. Effects of Vertical Conduction on Wardroom Bulkhead Temperatures

Upper and lower bulkhead temperatures (open and closed symbols, respectively) for the cases of no vertical conduction, conduction between the Laundry Room (compartment 1) and the Wardroom (compartment 3) and conduction between the Laundry Passageway (compartment 2) and the Wardroom. Two different areas were used for the exit vent for the no-conduction cases; only the smaller vent was used for those cases in which conduction was enabled.

3.4 The Navigation Equipment Room

The complex shape of the Navigation Equipment Room (illustrated in Figure 20) made it necessary to calculate approximate dimensions for the compartment. As in previous cases, a fictitious material (SHIPNER) had to be created to account for the differences among bulkheads. Previously, we only needed to determine the effective thickness of this virtual material but this case was much more complex because the bulkheads differed not only in thickness, but also in materials.

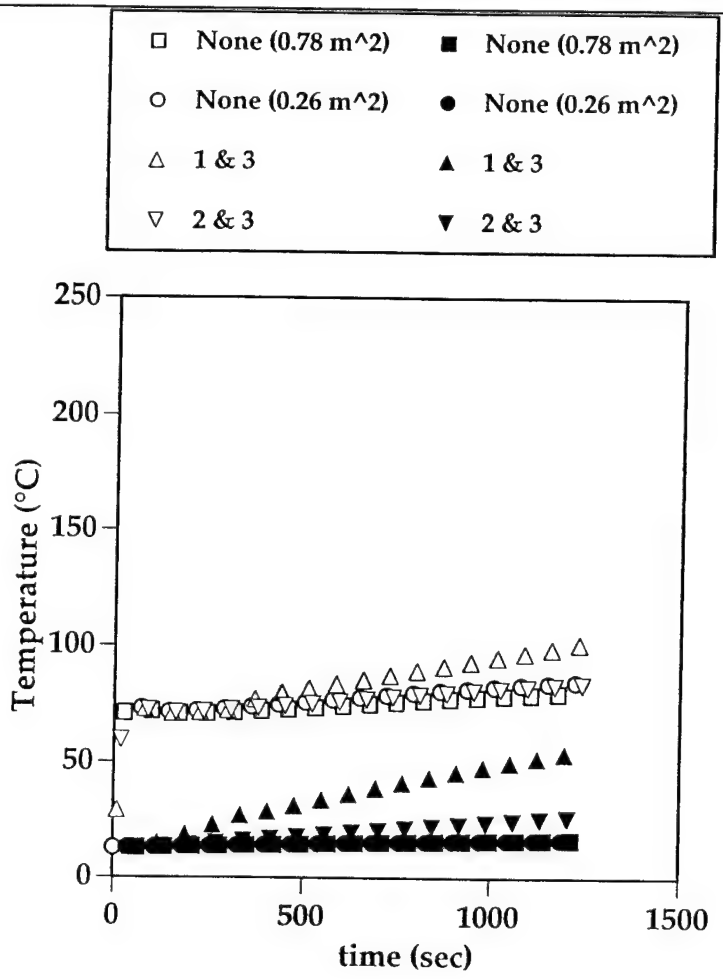

Figure 18. Effects of Vertical Conduction on Wardroom Gas Temperatures

Upper and lower layer gas temperatures (open and closed symbols, respectively) for the cases of no vertical conduction, conduction between the Laundry Room (compartment 1) and the Wardroom (compartment 3) and conduction between the Laundry Passageway (compartment 2) and the Wardroom. Two different areas were used for the exit vent for the no-conduction cases; only the smaller vent was used for those cases in which conduction was enabled.

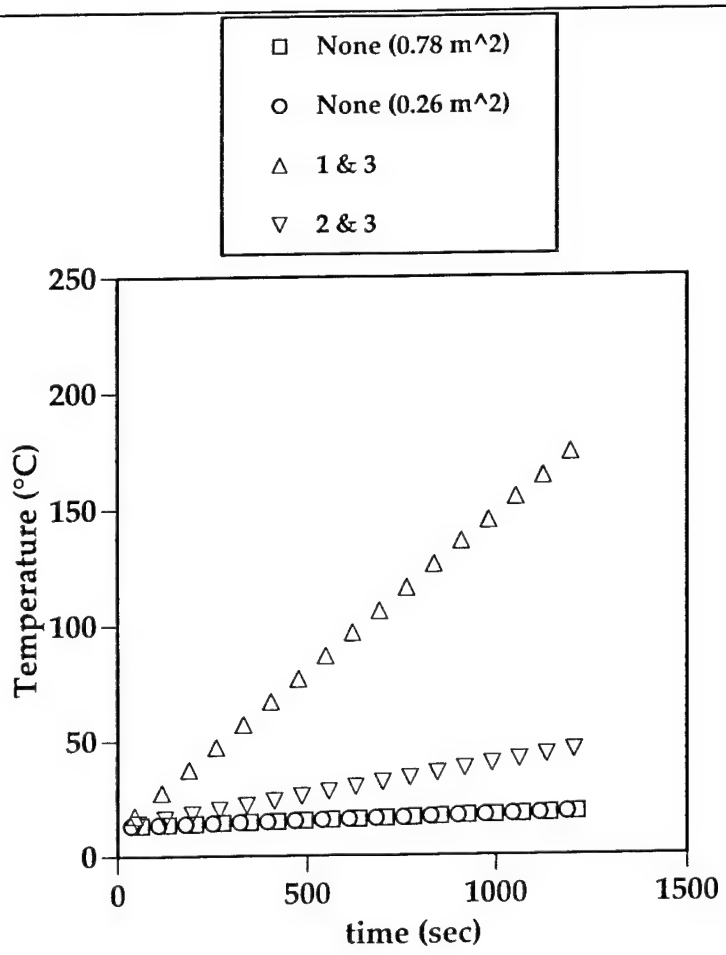

Figure 19. Effects of Vertical Conduction on Wardroom Deck Temperature

Deck temperatures for the cases of no vertical conduction, conduction between the Laundry Room (compartment 1) and the Wardroom (compartment 3) and conduction between the Laundry Passageway (compartment 2) and the Wardroom. Two different areas were used for the exit vent for the no-conduction cases; only the smaller vent was used for those cases in which conduction was enabled. Vertical conduction most strongly affects the deck temperature and this effect is most pronounced when the conduction is directly from the fire compartment.

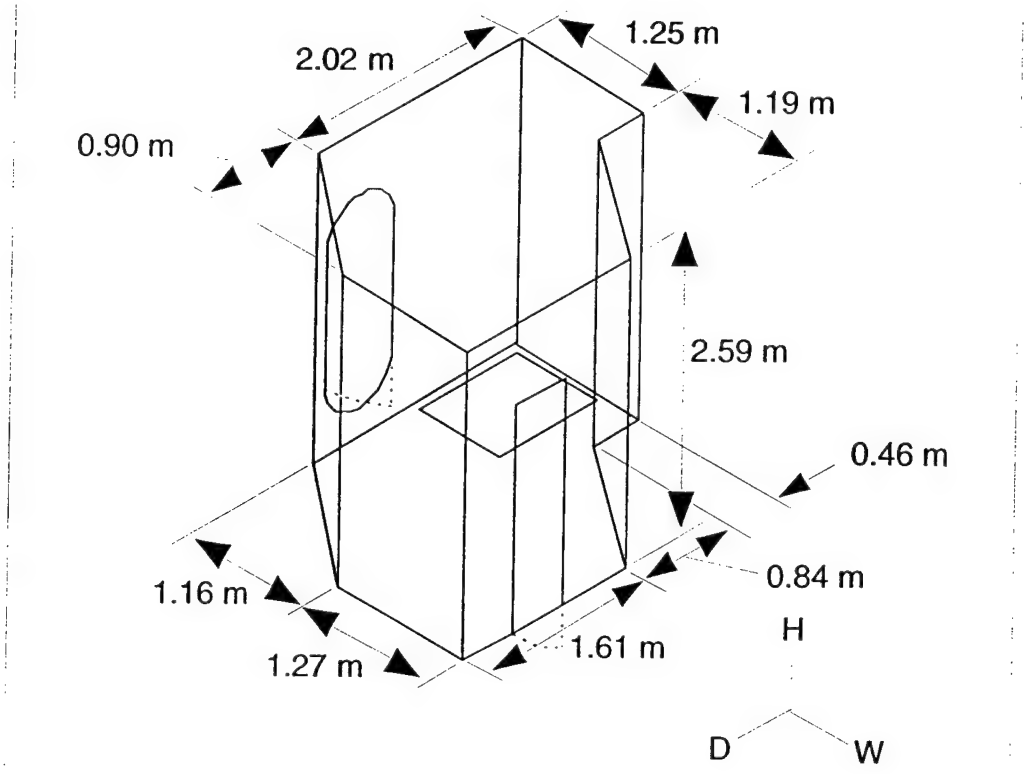

Figure 20. Navigation Equipment Room Dimensions

In addition to having a complex shape, the bulkhead between the Navigation Equipment Room and the Control Room was made of plywood rather than steel.

The forward bulkhead (on the right in the figure), was built of plywood to emulate a divider wall that exists between the Navigation Equipment Room and the Control Room on an actual LOS ANGELES class submarine. All of the original bulkheads were composed of various thicknesses of steel. Since the thermal conductivities, heat capacities and densities of steel and plywood are vastly different, we had to devise methods for calculating mean property values for our material. The fundamental problem was that it was not immediately obvious what weighting factors to use in order to calculate meaningful average values.

As before, we used an area-weighted mean thickness. For the conductivity, we wanted the effective heat flux, Q, to be equal to the sum of the heat fluxes, Q_i, through the various pieces of the bulkhead

$$Q = \sum Q_i \qquad \text{Eqn. 24}$$

or, in terms of the material properties

$$\kappa A \Delta T / t = \sum \kappa_i A_i \Delta T_i / t_i \qquad \text{Eqn. 25}$$

where κ, A and t are the conductivities, areas and thicknesses of the materials and ΔT_i is the temperature difference across the thickness for each section. Each part of the real bulkhead may have a different ΔT_i and, since those values are time dependent, we can not calculate a constant value for the effective conductivity.

Recall, however, that the current version of CFAST treats walls as if they were a single entity that wraps around the compartment. Due to this limitation, CFAST acts as though all of the ΔT_i values were the same. Consequently, we introduce no additional error if we also treat ΔT_i as constant. Using this approximation, we can cancel the temperature terms on both sides of the equation and, solving for κ, we get

$$\kappa = \sum \kappa_i (A_i / A) (t / t_i) \qquad \text{Eqn. 26}$$

The mass of our virtual bulkheads should be equal to the total mass of the real bulkheads which, using the same approach, gives us

$$\rho = \sum \rho_i (A_i / A) (t_i / t) \qquad \text{Eqn. 27}$$

Similarly, the requirement for equal heat content of the bulkheads leads to

$$C = \sum C_i \ (\rho_i / \rho) (A_i / A) (t_i / t) \qquad \text{Eqn. 28}$$

3.4.1 Characteristics of the Navigation Equipment Room

The first step was to subdivide the deck into three parts, shown in Figure 21, each of which was a trapezoid[11]. Using the dimensions from the figure, the deck area was then

$$A_{deck} = A_1 + A_2 + A_3 = 5.55 \text{ m}^2 \qquad \text{Eqn. 29}$$

For consistency with the Control Room, we used the actual height, 2.59 m, and the mean depth of Part 2 (2.92 m) as the effective height and depth, respectively. The effective width was then calculated as

$$W_{eff} = A_{deck} / D_{eff} = 1.90 \text{ m} \qquad \text{Eqn. 30}$$

The Navigation Equipment Room bulkhead was divided into seven segments, indicated by the circled numbers in Figure 21. The areas for each bulkhead segment, and for the complete bulkhead, were calculated using the segment lengths from Figures 20 and 21 and the compartment height. The area-weighted thickness was then calculated and, with this information, we were able to determine all of the weighting factors for Equations 26 - 28. Property values for steel and plywood were taken from CFAST's standard Thermal.df materials database (Table 4) and the results of these calculations are shown in Table 5.

[11] The slightly different depths for the fore and aft edges of Part 2 were due to the taper of the hull.

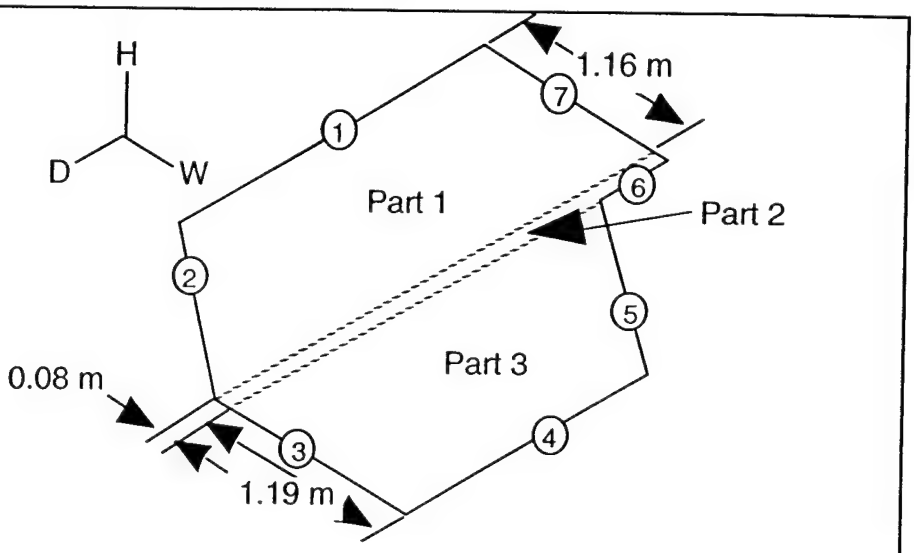

Figure 21. Navigation Equipment Room Deck

The deck area divided was into three regions, designated as Parts 1 - 3, and the total area was calculated as the sum of the three trapezoids. The numbers in circles correspond to the bulkhead segments listed in Table 5

Material	Conductivity (W/m K)	Heat Capacity (J/kg K)	Density (kg/m^3)
Steel	48	559	7854
Plywood	0.12	1215	545

Table 4. Standard Thermal.df Entries for Steel and Plywood

Bulkhead Segment	Area (m^2)	Thick (m)	(A_i/A)	$(A_i/A)t_i$
1	5.23	0.0095	0.2117	0.0020
2	3.81	0.0095	0.1542	0.0015
3	3.29	0.0095	0.1331	0.0013
4*	4.17	0.0127	0.1688	0.0021
5*	3.78	0.0127	0.1530	0.0019
6*	1.19	0.0127	0.0482	0.0006
7	3.24	0.0095	0.1311	0.0012
Totals	24.71			0.0106

Table 5. Calculation of Thermal Properties for SHIPNER

Bulkhead segments were numbered counterclockwise, starting from the aftmost segment, as shown in Figure 21. Segments marked with * are plywood; the others are steel.

Bulkhead Segment	(t_i/t)	$(A_i t/A t_i)\kappa_i$	$(A_i t_i/At)\rho_i$	$(A_i t_i \rho_i/At\rho)C_i$
1*	0.8962	11.34	1490	178
2*	0.8962	8.26	1085	130
3*	0.8962	7.13	937	112
4	1.1981	0.0169	110	29
5	1.1981	0.0153	100	26
6	1.1981	0.0048	31	8
7*	0.8962	7.02	923	110
Totals		33.79	4676	593

Table 5 (Cont'd). Calculation of Thermal Properties for SHIPNER

The model ran successfully using the above dimensions, the SHIPNER material properties and a one-third scale Wardroom-Navigation Equipment Room vent. We then tried replacing that vent with one of the correct size and found that the model continued to work. Accordingly, the full-size vent was used for the next phase.

3.5 The Control Room

The Control Room, illustrated in Figure 22, was similar in shape to the Navigation Equipment Room and shared a plywood bulkhead with the latter compartment. The same methods were used

to calculate the model dimensions and thermal parameters for both compartments. For the Control Room, the bulkhead material was named SHIPCR.

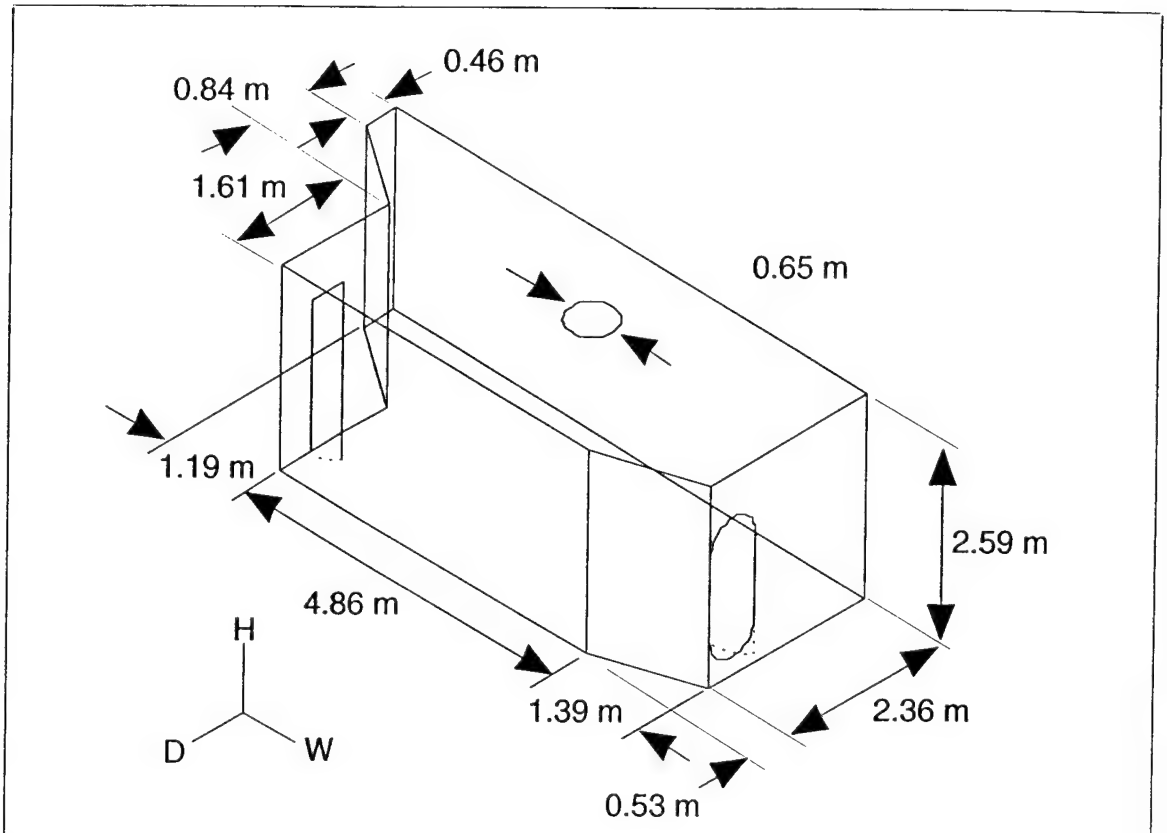

Figure 22. Control Room Dimensions

The Control Room was similar to the Navigation Equipment Room, although much larger, and the two compartments shared a plywood bulkhead

3.5.1 Characteristics of the Control Room

As in the previous compartment, the deck area was calculated as the sum of three trapezoids (shown in Figure 23); the actual height was used and the effective depth was the mean depth of the central portion of the deck. The model dimensions were then

$$H_{eff} = 2.59 \text{ m} \qquad \text{Eqn. 31a}$$

$$D_{eff} = 2.90 \text{ m} \qquad \text{Eqn. 31b}$$

$$W_{eff} = 6.30 \text{ m} \qquad \text{Eqn. 31c}$$

Unlike the previous vertical vents, the vent from this compartment to the Sail was circular (Type 1) and had an area of 0.33 m^2. Vertical conduction from the Wardroom to the Control Room was

enabled[12] and the materials properties shown in Table 6 were used for SHIPCR. With these parameters, we were able to successfully run the model.

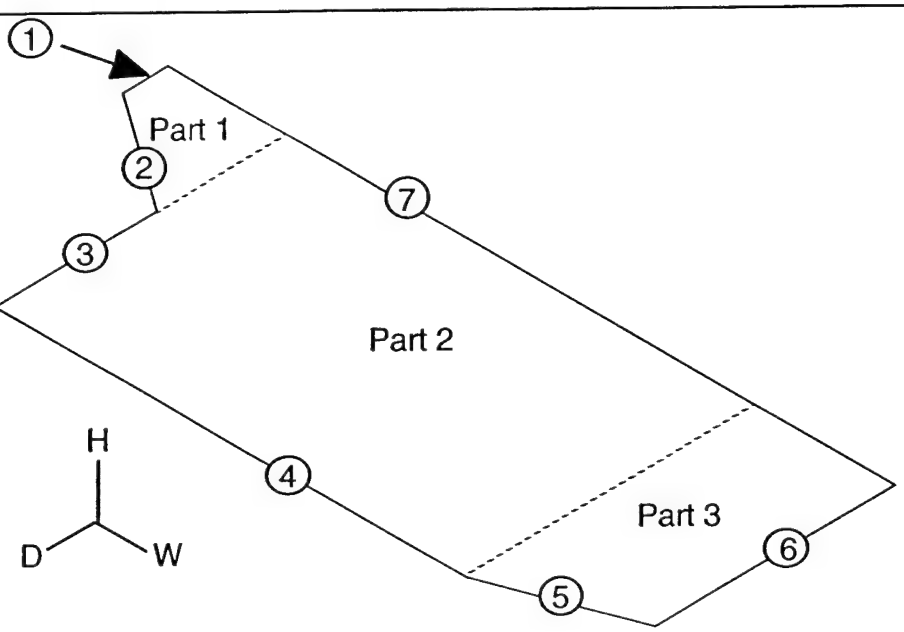

Figure 23.Control Room Deck

Like the Navigation Equipment Room, the Control Room deck area was calculated as the sum of three trapezoids. The numbers in circles correspond to the bulkhead segments listed in Table 6.

Bulkhead Segment	Area (m^2)	Thick (m)	(A_i/A)	$(A_i/A)t_i$
1*	1.19	0.0127	0.0238	0.0003
2*	3.78	0.0127	0.0756	0.0010
3*	4.17	0.0127	0.0833	0.0011
4	12.12	0.0095	0.2423	0.0023
5	3.86	0.0095	0.0772	0.0007
6	6.11	0.0095	0.1221	0.0012
7	18.80	0.0095	0.3758	0.0036
Totals	50.03			0.0102

Table 6. Calculation of Thermal Properties for SHIPCR

Bulkhead segments were numbered counterclockwise, starting from the aftmost segment, as shown in Figure 23. Segments marked with * are plywood; the others are steel.

[12] We chose to specify conduction to the Control Room, rather than to the Navigation Equipment Room, because the deck area of the former was approximately three times greater and we therefore expected the majority of the conductive transport to occur between the Wardroom and the Control Room.

Bulkhead Segment	(t_i/t)	$(A_i t/A t_i)\kappa_i$	$(A_i t_i/At)\rho_i$	$(A_i t_i \rho_i/At\rho)C_i$
1*	1.2451	0.0023	16	3
2*	1.2451	0.0073	51	10
3*	1.2451	0.0080	57	11
4	0.9314	12.49	1772	162
5	0.9314	3.98	565	52
6	0.9314	6.29	893	82
7*	0.9314	19.37	2749	252
Totals		42.14	6103	572

Table 6 (Cont'd). Calculation of Thermal Properties for SHIPCR

3.6 The Sail

The Sail is not part of a submarine's pressure hull — it is primarily a streamlined fairing that protects a variety of sensors (periscopes, radar and electronic countermeasures systems, for example). The only portion that is accessible from inside the ship is an access trunk which leads to a navigation watch station platform near the top of the Sail. For fire modeling purposes, this access trunk is the only part in which we are interested.

The access trunk is composed of two parts, shown in Figure 24. The lower section has an elliptical cross-section while the upper portion is circular. This arrangement suggests that we could apply the virtual compartment method (previously discussed for the Laundry Passageway) and treat the Sail as if it were two compartments. Alternatively, we could have modeled it as a single compartment having the same total volume as the two sections. We chose the former because it provided a better representation of the actual geometry with fewer approximations. The lower section was designated Sail_1 and the upper was Sail_2.

Since CFAST can not directly handle compartments having curved bulkheads, we had to approximate both sections of the Sail as if they were rectangular. Actual heights were used for both and the deck area was calculated using the formula for an ellipse

$$A_{deck} = \pi ab \qquad \text{Eqn. 32}$$

(where a and b are the semiaxes) and a circle, respectively. For the lower section, the effective depth was assumed to be equal to the maximum depth of the ellipse. In the case of the upper section, we approximated the circular deck as a square of the same area.

Like the Navigation Equipment Room and the Control Room, the Sail was not part of the original ship's structure and had been added specifically for fire tests. Since the materials for the access tunnel were not specified in the test descriptions, we assumed them to be the same as the steel components of the Navigation Equipment Room and Control Room, 0.952 cm (0.375 in.) steel. This is one of the standard materials in the database, so no fictitious material was needed for the Sail.

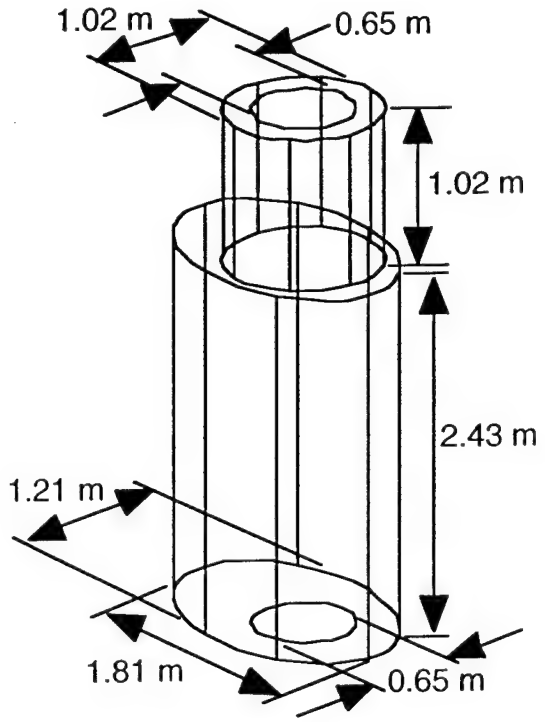

Figure 24. Sail Dimensions

The Sail was modeled as two separate compartments, one above the other. Because CFAST can not represent curved, both of these had to be approximated as having rectangular boundaries.

3.6.1 Characteristics of the Sail

Based on the above, the dimensions were

$$H_{eff} = 2.43 \text{ m} \quad \text{Eqn. 33a}$$

$$D_{eff} = 1.21 \text{ m} \quad \text{Eqn. 33b}$$

$$W_{eff} = A_{deck} / D_{eff} = 1.42 \text{ m} \quad \text{Eqn. 33c}$$

for the lower section and

$$H_{eff} = 1.02 \text{ m} \quad \text{Eqn. 34a}$$

$$W_{eff} = D_{eff} = 0.91 \text{ m} \quad \text{Eqn. 34b}$$

for the upper.

Conduction was used between the Control Room and the lower portion of the Sail. However, because the entire deck area of Sail_2 was a vertical vent, conduction between two sections of the Sail was not enabled. The opening between the two sections was specified as a circular vent having an area of 0.82 m^2 and the vent from the upper section to the outside was the same as the Control Room hatch. No adjustments to these values were needed in order to get the simulation to run to completion.

The final SHADWELL/688 model is given in Listing 3, which includes the fire, as well as the geometry, specification.

```
VERSN     3 SHADWELL/688 Laundry - Sail.
#        Sim.time   Print   Hist.   Disp.   Copies
TIMES      1250       1       3       0       0
#         Temp.      Press.      Elev.
TAMB    285.900    101300.    0.000000
EAMB    286.300    101300.    0.000000
#
#      Cmpt. 1  Cmpt. 2  Cmpt. 3  Cmpt. 4  Cmpt. 5  Cmpt. 6  Cmpt. 7
#      Laundry  Psgwy    Wardrm   NER      CR       Sail_1   Sail_2
#Floor elevation
HI/F    0.00     0.00     2.57     5.16     5.16     7.75     10.18
#X dimen.
DEPTH   1.75     10.26    4.00     2.92     2.90     1.21     0.91
#Y dimen.
WIDTH   6.07     2.22     8.51     1.90     6.30     1.42     0.91
#Z dimen.
HEIGH   2.57     2.57     2.59     2.59     2.59     2.43     1.02
#
#Materials
CEILI   SHIP3/8  SHIP3/8  SHIP7/8  SHIP3/8  SHIP3/8  SHIP3/8  SHIP3/8
WALLS   SHIPLR   SHIPLRP  SHIPWR   SHIPNER  SHIPCR   SHIP3/8  SHIP3/8
FLOOR   SHIP3/8  SHIP3/8  SHIP3/8  SHIP7/8  SHIP7/8  SHIP3/8  SHIP3/8
```

Listing 3. Input File for the Final SHADWELL/688 Simulation

```
#Laundry-Passageway door
#      Cmpt#    Cmpt#    Vent#    Width     Soffit     Sill     Wind
HVENT  1        2        1        0.66      1.90       0.00     0.00
#      Cmpt#    Cmpt#    Vent#    Width@t0  Width@t1
CVENT  1        2        1        1.00      1.00
#
#Passageway-AMR door
#      Cmpt#    Cmpt#    Vent#    Width     Soffit     Sill     Wind
HVENT  2        8        1        0.66      2.04       0.23     0.00
#      Cmpt#    Cmpt#    Vent#    Width@t0  Width@t1
CVENT  2        8        1        1.00      1.00
#
#Passageway-Torpedo Rm door
#      Cmpt#    Cmpt#    Vent#    Width     Soffit     Sill     Wind
HVENT  2        8        2        0.66      2.04       0.23     0.00
#      Cmpt#    Cmpt#    Vent#    Width@t0  Width@t1
CVENT  2        8        2        1.00      1.00
#
#Passageway-Wardroom hatch
#      Cmpt#    Cmpt#    Area     Type (1 = circular; 2 = square)
VVENT  2        3        0.78       2
#
#Wardroom-Crew Mess door
#      Cmpt#    Cmpt#    Vent#    Width     Soffit     Sill     Wind
HVENT  3        8        1        0.66      2.04       0.23     0.00
#      Cmpt#    Cmpt#    Vent#    Width@t0  Width@t1
CVENT  3        8        1        1.00      1.00
#
#Wardroom-Crew Living door
#      Cmpt#    Cmpt#    Vent#    Width     Soffit     Sill     Wind
HVENT  3        8        2        0.66      2.04       0.23     0.00
#      Cmpt#    Cmpt#    Vent#    Width@t0  Width@t1
CVENT  3        8        2        1.00      1.00
#
#Wardroom-Nav. Equip. Rm. hatch
#      Cmpt#    Cmpt#    Area     Type (1 = circular; 2 = square)
VVENT  3        4        0.78       2
#
#Laundry-Wardroom heat conduction
#      Cmpt#    Cmpt#
CFCON    1      3
#
#Nav. Equip. Rm-Fan Rm. door
#      Cmpt#    Cmpt#    Vent#    Width     Soffit     Sill     Wind
HVENT  4        8        1        0.66      2.04       0.23     0.00
#      Cmpt#    Cmpt#    Vent#    Width@t0  Width@t1
CVENT  4        8        1        1.00      1.00
#
#Nav. Equip. Rm.-Control Rm. door
#      Cmpt#    Cmpt#    Vent#    Width     Soffit     Sill     Wind
HVENT  4        5        1        0.50      1.92       0.00     0.00
#      Cmpt#    Cmpt#    Vent#    Width@t0  Width@t1
CVENT  4        5        1        1.00      1.00
#
```

Listing 3. Input File for the Final SHADWELL/688 Simulation

```
#Control Rm.-Combat Systems door
#      Cmpt#    Cmpt#    Vent#    Width     Soffit     Sill     Wind
HVENT  5        8        1        0.66      2.04       0.23     0.00
#      Cmpt#    Cmpt#    Vent#   Width@t0  Width@t1
CVENT  5        8        1       1.00      1.00
#
#Control Rm.-Sail_1 hatch
#      Cmpt#    Cmpt#    Area    Type (1 = circular; 2 = square)
VVENT  5        6        0.33      1
#
#Wardroom-Control Rm. heat conduction
#      Cmpt#    Cmpt#
CFCON   3       5
#
#Sail_1-Sail_2 opening
#      Cmpt#    Cmpt#    Area    Type (1 = circular; 2 = square)
VVENT  6        7        0.82      1
#
#Control Rm.-Sail_1 heat conduction
#      Cmpt#    Cmpt#
CFCON   5       6
#
#Sail_2-Exterior opening
#      Cmpt#    Cmpt#    Area    Type (1 = circular; 2 = square)
VVENT  7        8        0.33      1
#
#Fire position
FPOS   0.91  1.83  0.19
#Fire Cmpt
LFBO       1
#Fire Type (1 = unconstrained; 2 = constrained)
LFBT       2
#                 t0        t1
FTIME                      1250.
#Mass pyrolysis rate
FMASS           0.0253    0.0229
#       Mol Wt    Rel Hum    LOL        Hc       Init T    Ign. T   Rad. fract.
CHEMI    184.       100.     10.   4.19E+007     285.9      330.      0.30
#H:C mass ratio (fuel composition)
HCR             0.143      0.143
#O:C mass ratio (fuel composition)
O2              0.0        0.0
#Soot:CO2 mass ratio (combustion)
OD              0.06       0.06
#CO:CO2 mass ratio (combustion)
CO              0.056      0.056
#HCN:fuel mass ratio (pyrolysis)
HCN             0.0        0.0
#HCl:fuel mass ratio (pyrolysis)
HCL             0.0        0.0
#Toxics:fuel mass ratio (pyrolysis)
CT              0.0        0.0
CJET OFF
DUMPR model.HI
```

Listing 3 (cont'd). Input File for the Final SHADWELL/688 Simulation

4.0 COMPARISON WITH EXPERIMENTAL RESULTS

Using the complete SHADWELL/688 model, as described in the preceding section, we were able to produce predictions that could be compared with the existing data set. As was previously mentioned, CFAST-predicted interface heights were used to determine which thermocouples were in the upper layer and which were in the lower layer for each compartment.

As a practical matter, the interface heights were not constant over the duration of the simulations. Typically, they change rapidly in the first minute and then very slowly for the remainder of the time (Figure 25). Since it was not practical to apportion sensors on a second-by-second basis, we have used the mean of the interface heights at 60 and 1250 seconds. These times were arbitrary, but approximately represented the period over which the interface height was nearly constant.

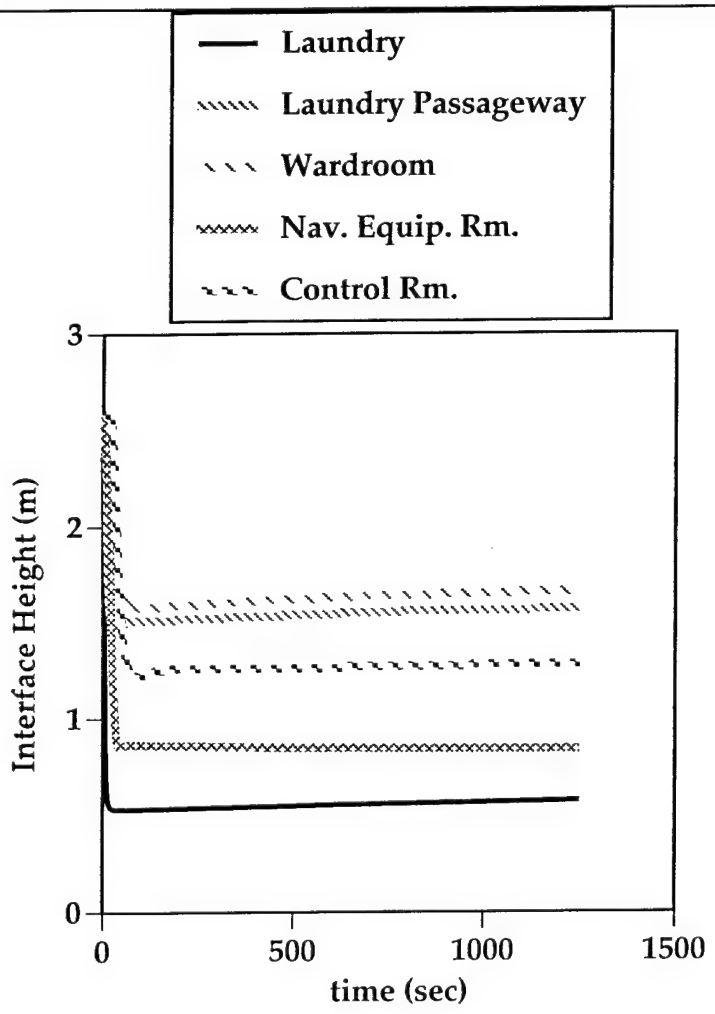

Figure 25. CFAST-Predicted Interface Heights

For each time, CFAST calculates the height of the boundary between the upper and lower gas layers. This value is also used as the demarcation between the upper and lower walls.

For each compartment, the thermocouples were then categorized as being in the upper or lower layer, depending on whether they were above or below this interface. Table 7 gives the interface values used and the number of thermocouples in each layer for each compartment. We did not consider the Sail because there was only a single thermocouple in the entire access trunk.

Cmpt.	Interface Ht (m)	Upper TCs	Lower TCs
Laundry	0.56	4	2
Passageway	1.54	2	4
Wardroom	1.64	9	20
Nav. Equip.	0.85	4	2
Control Rm.	1.30	6	7

Table 7. Interface Heights and Apportionment of Thermocouples

The interface height, as predicted by CFAST, was used to determine which thermocouples were in the upper and lower layers.

As we see in Figures 26 and 27, there is excellent agreement between the predicted and actual air temperatures for the Laundry Room itself. In the case of the Laundry Passageway (Figures 28 and 29), both layers are under predicted, although only by about one standard deviation for the lower layer. Only two thermocouples were in the upper layer and they were both located close to the aft end of the compartment, exposed to the gas jet from the Laundry Room and far from the overhead vent leading to the Wardroom. As a consequence, those two thermocouples probably were not a good sample of the upper layer temperatures throughout the compartment.

In contrast, there were 29 thermocouples in the Wardroom, comprising five different thermocouple trees. Three of these were located in the forward quarter of the compartment and two in the aft quarter, so it is likely that these measurements were reasonably representative of average compartment temperatures. For this compartment, CFAST seriously overestimated the air temperatures, as illustrated in Figure 30 (upper layer) and Figure 31 (lower layer).

Looking at the upper layer of the Navigation Equipment Room (Figure 32), we see that there is fairly good agreement between the model and the test. However, given the major discrepancy in the upper layer temperatures for the Wardroom, any agreement in the Navigation Equipment Room should be considered to have been fortuitous. This is reinforced by the observation that the predicted lower layer temperature for this compartment shows a negligible increase above the pre-fire condition (Figure 33). Clearly, a jet of superheated gas (from the upper layer of the Wardroom) could not rise through the lower layer of the Navigation Equipment Room without heating that layer.

The situation in the Control Room (Figures 34 and 35) is similar to that seen in the previous compartment — no noticeable increase in the predicted lower layer, resulting in very poor agreement with experiment, and surprisingly good agreement with the data for the upper layer.

5.0 CONCLUSIONS

We have demonstrated that, using CFAST, it is possible to build a model for a complex, multi-compartment shipboard fire scenario using the information that would be available to ship designers. In our first report [2], we showed that a fire specification could be created based largely on fuel and combustion properties obtained from the literature or estimated from prior experience with CFAST fire modeling. In this report, the geometrical specifications have been developed from a knowledge of the actual ship configuration.

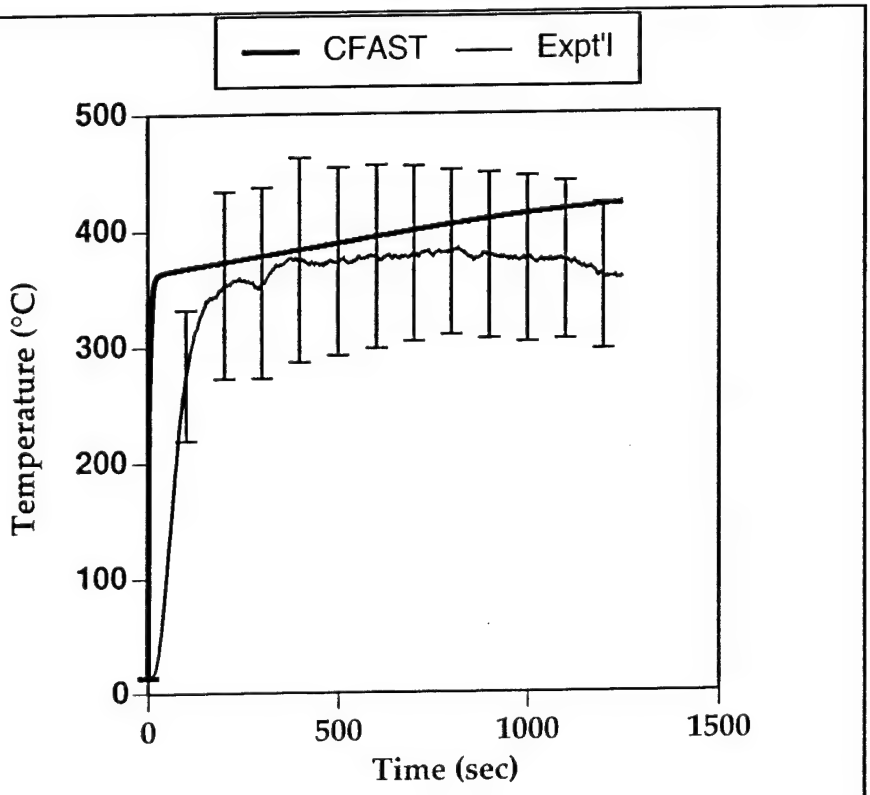

Figure 26. Predicted versus Measured Upper Layer Gas Temperatures for the Laundry Room

These experimental temperatures are the mean of four thermocouples. The error bars represent one standard deviation. Compare with Figure 5 to see the effects of adding additional compartments to the original Laundry Room model.

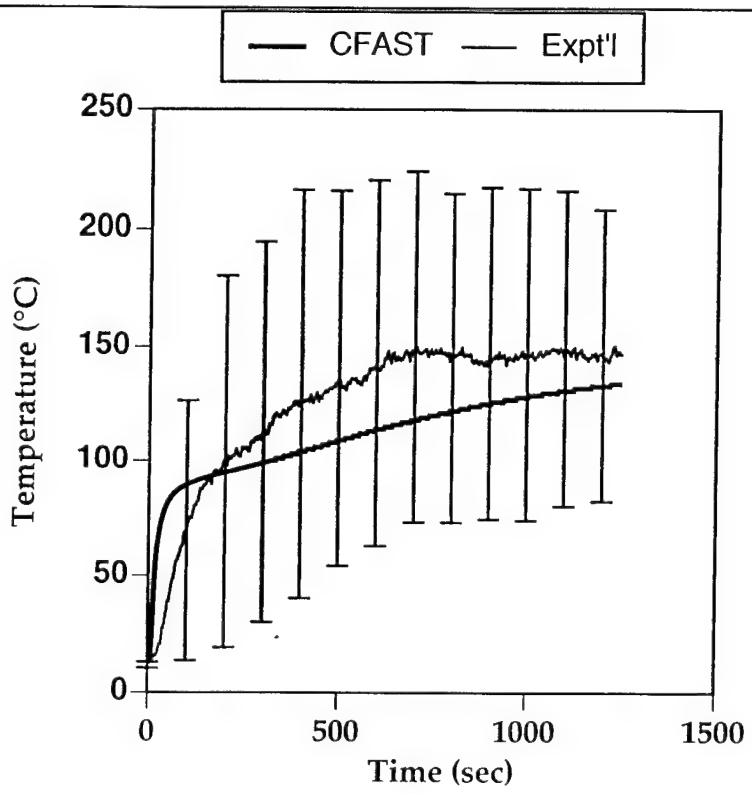

Figure 27. Predicted versus Measured Lower Layer Gas Temperatures for the Laundry Room

These experimental temperatures are the mean of two thermocouples. The error bars represent one standard deviation. Compare with Figure 6 to see the effects of adding additional compartments to the original Laundry Room model.

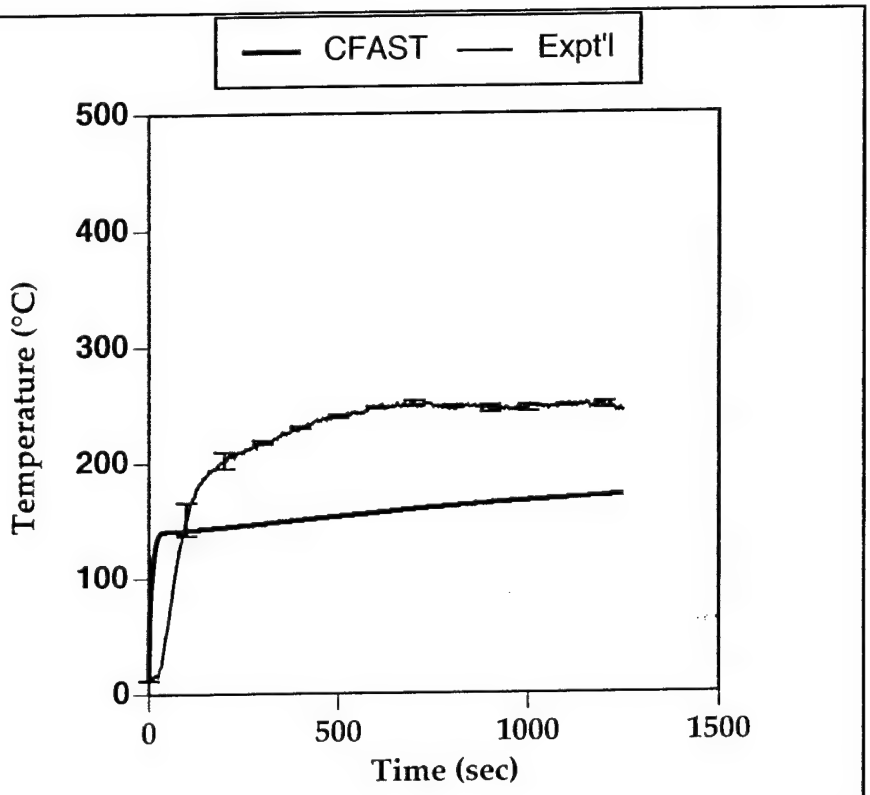

Figure 28. Predicted versus Measured Upper Layer Gas Temperatures for the Laundry Passageway

These experimental temperatures are the mean of two thermocouples. The error bars represent one standard deviation.

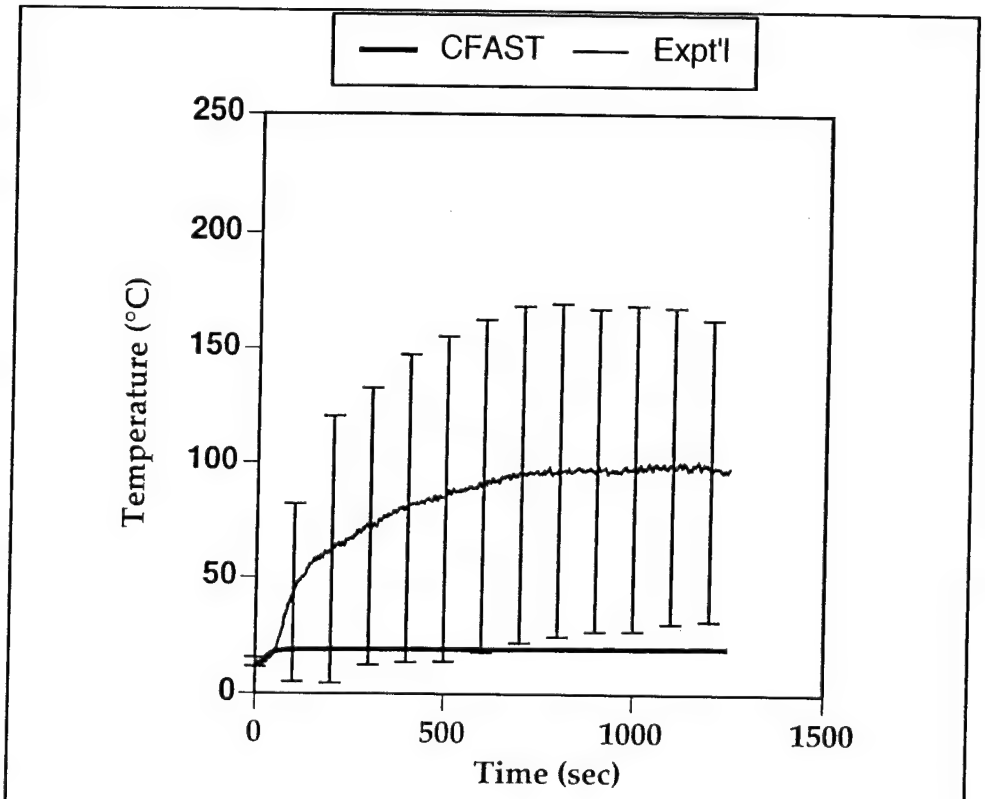

Figure 29. Predicted versus Measured Lower Layer Gas Temperatures for the Laundry Passageway

These experimental temperatures are the mean of four thermocouples. The error bars represent one standard deviation.

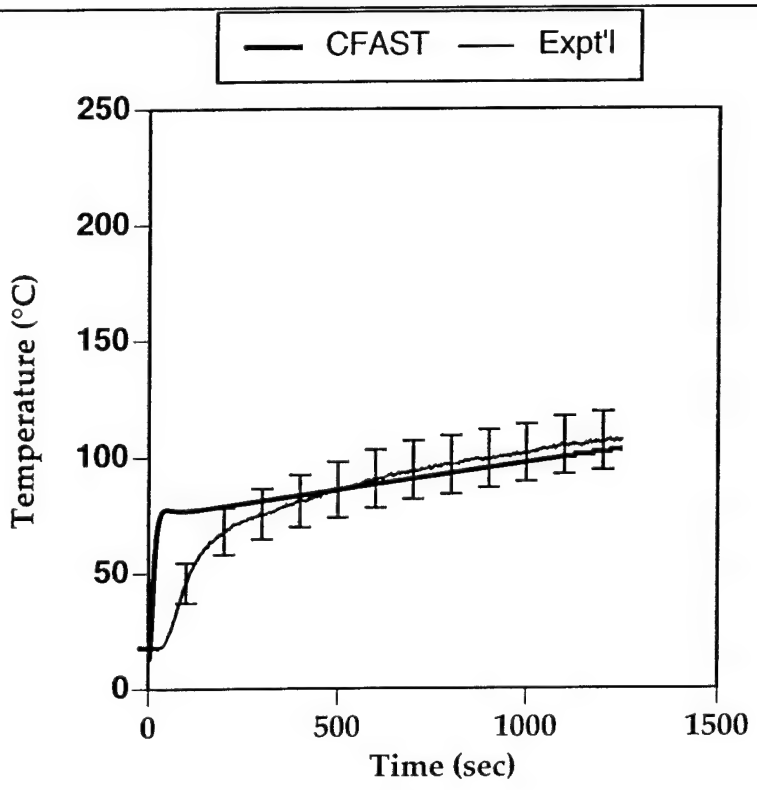

Figure 30. Predicted versus Measured Upper Layer Gas Temperatures for the Wardroom

These experimental temperatures are the mean of nine thermocouples. The error bars represent one standard deviation.

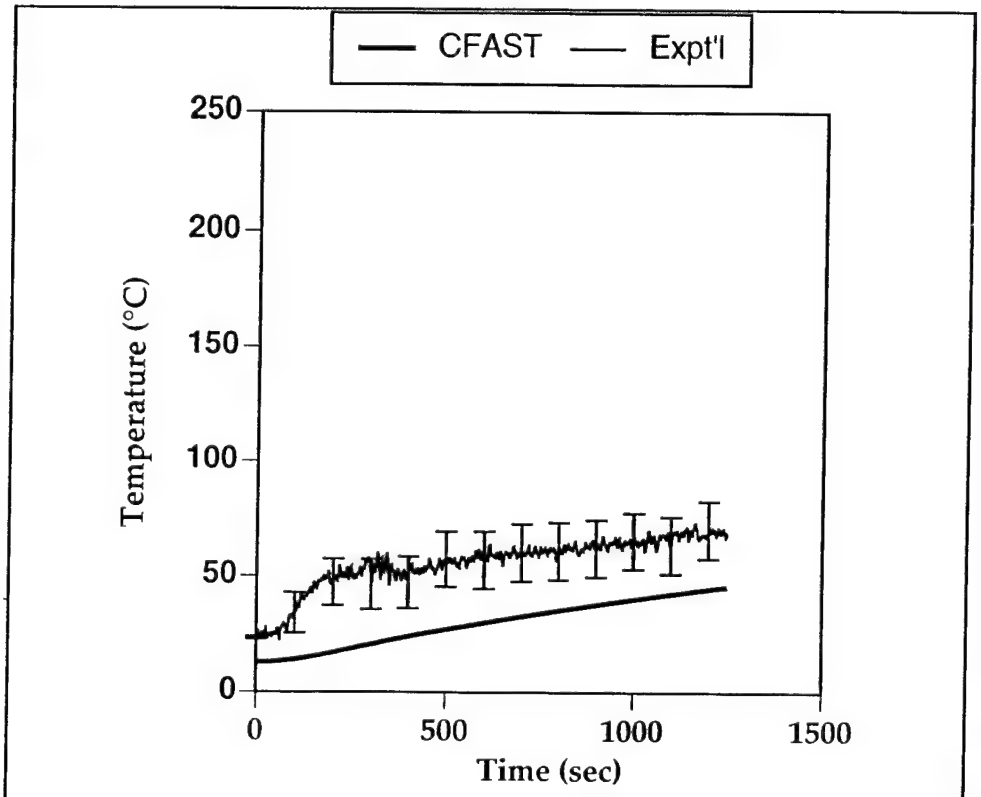

Figure 31. Predicted versus Measured Lower Layer Gas Temperatures for the Wardroom

These experimental temperatures are the mean of 20 thermocouples. The error bars represent one standard deviation.

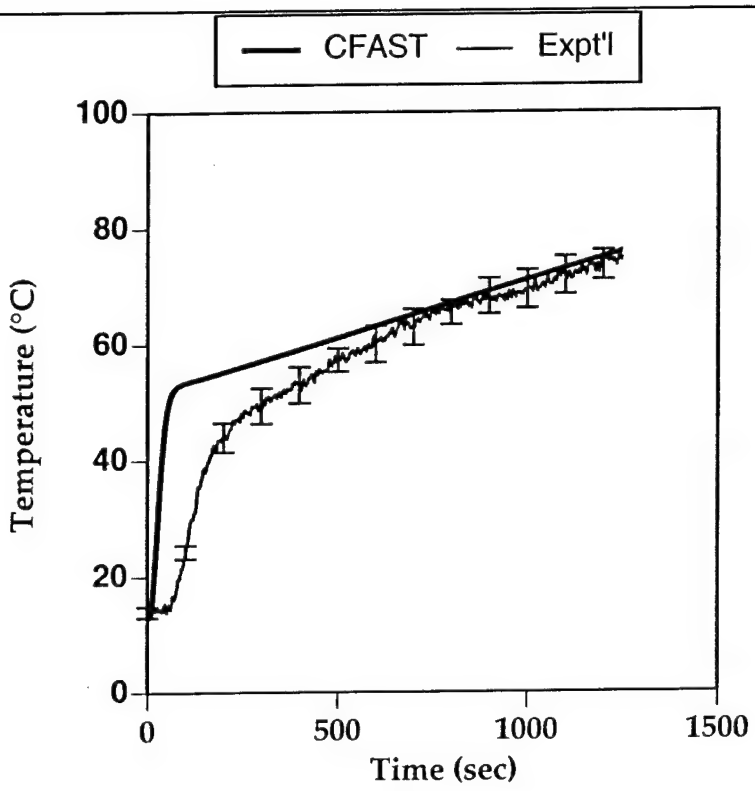

Figure 32. Predicted versus Measured Upper Layer Gas Temperatures for the Navigation Equipment Room

These experimental temperatures are the mean of four thermocouples. The error bars represent one standard deviation.

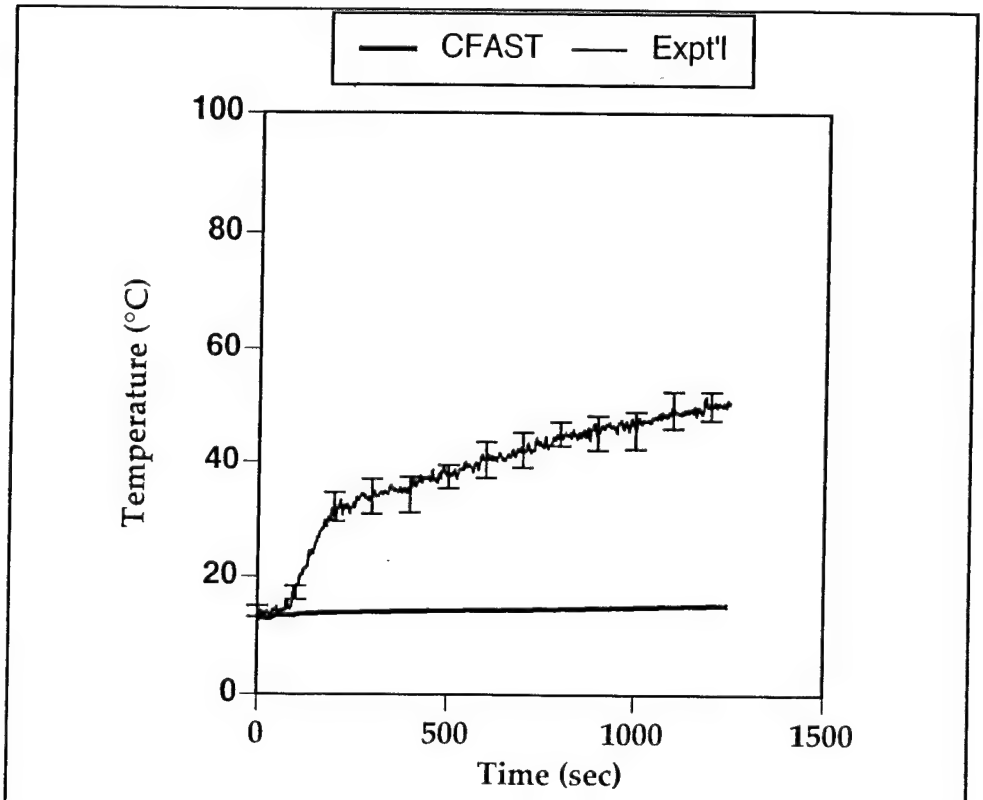

Figure 33. Predicted versus Measured Lower Layer Gas Temperatures for the Navigation Equipment Room

These experimental temperatures are the mean of two thermocouples. The error bars represent one standard deviation.

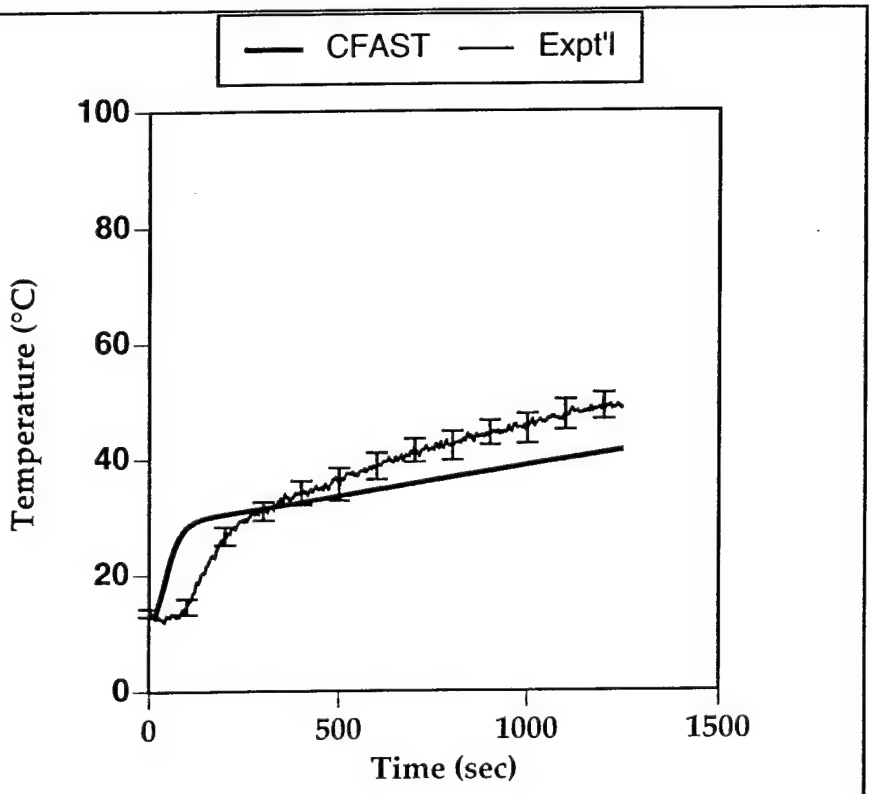

Figure 34. Predicted versus Measured Upper Layer Gas Temperatures for the Control Room

These experimental temperatures are the mean of six thermocouples. The error bars represent one standard deviation.

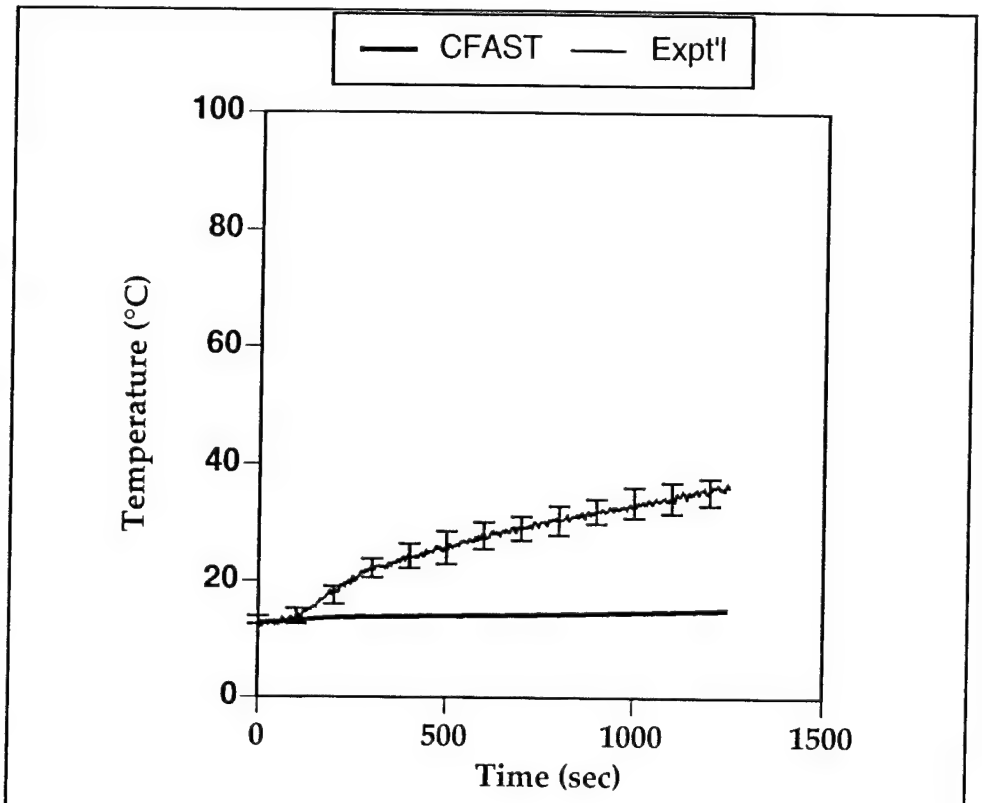

Figure 35. Predicted versus Measured Lower Layer Gas Temperatures for the Control Room

These experimental temperatures are the mean of seven thermocouples. The error bars represent one standard deviation.

Due to the inherent limitations of the CFAST vocabulary, we knew that it would not be possible to directly represent most ship compartments. However, we have shown that it is possible to describe even complex compartments using reasonable approximations. The techniques for this have included subdividing compartments and reassembling the pieces to produce a simplified compartment and the use of multiple virtual compartments to represent a single real compartment.

During this process, we found that some situations could not be represented at all (for example, it is not possible for one compartment to simultaneously conduct heat through the overhead into two different compartments) and that specific combinations of input parameters could cause the CFAST to slow to the point of being effectively unusable. There in no known way to predict which input combinations will cause the latter problem or for what ranges of variables this problem will occur.

The suggested approach to resolving this type of problem is to adjust parameter values until the model runs successfully, then fine tune the parameters to be as close to reality as possible without causing CFAST to stall. For this reason, it has been found to be very advantageous to build a complex model by starting with a simple, working case and adding features, one at a time, until the desired scenario is reached. Experience has shown that attempts to construct complex cases from scratch are usually doomed to failure.

We have found that, when adding compartments to a model, feedback effects can significantly alter the behavior of pre-existing parts of the model. Thus, if the desired combination of parameters will not work, it is possible that the addition of another compartment will permit the model to run. In several cases, this allowed us to improve the model by using the correct size for a vertical vent when, in the absence of the new compartment, that size vent would not work.

Agreement between the model and experiment was excellent for the fire compartment, but not very good for other compartments. In the case of the Laundry Passageway, there was little data for comparison and there is reason to believe that the data that were available may not have been representative of the entire compartment.

For the other compartments, the discrepancy between model and data can not be explained away so easily. Both the Wardroom and the Control Room had large numbers of thermocouples (29 and 13, respectively) and the Navigation Equipment Room was very small so the six available thermocouples represented a reasonably high density of measurements.

Given that the temperatures in the fire compartment were correctly predicted, discrepancies in the other compartments must be due to problems in calculating mass or energy transport. Mass transport through horizontal vents, such as doors, has been a part of CFAST from the beginning and is not likely to be grossly in error. However, both vertical vent flow and vertical heat conduction are relatively recent additions to the model and one, or both, may have contributed to these results.

Several areas for further work have been identified. First, it would be very useful to more carefully investigate the behavior of vertical vent flow and vertical heat conduction since there is reason to suspect that they are significant factors in the deviation between theory and experiment. The algorithm for square vertical vents, in particular, appears to be somewhat fragile as we found that it caused problems in each compartment in which it was used. It is also notable that the Wardroom, which was the first compartment in which this algorithm was the controlling factor, shows the worst agreement with the test data.

We also note that, as we would expect, the data show a noticeable delay between ignition and the time that the compartment temperatures begin to rise in compartments far from the fire. In contrast, CFAST always predicts a near-instantaneous response to the fire, which is clearly non-physical (see Figure 34, for example). This is further support for our belief that there are important transport issues that need to be resolved before CFAST is used for mission-critical work.

6.0 ACKNOWLEDGMENTS

The work described in this report was performed by the Chemistry Division of the Materials Science and Component Technology Directorate, Naval Research Laboratory. The work was funded by the Office of Naval Research, Code 334, under the Damage Control Task of the FY99 Surface Ship Hull, Mechanical, and Electrical Technology Program (PE0602121N).

The authors wish to thank Jean Bailey (NRL Code 6183) for her assistance in performing the CFAST modeling.

7.0 REFERENCES

1. "CFAST, the Consolidated Model of Fire Growth and Smoke Transport", Richard D. Peacock, Glenn P. Forney, Paul Reneke, Rebecca Portier and Walter Jones, US Department of Commerce Technical Report TN 1299, 1993.

2. "Application of CFAST to Shipboard Fire Modeling I. Development of the Fire Specification", J. B. Hoover and P. A. Tatem, NRL Memo Report NRL/MR/6180--00-8466, 2000.

3. "Meta-Analysis of Data from the Submarine Ventilation Doctrine Test Program", J. B. Hoover, P. A. Tatem and F. W. Williams, NRL Memo Report NRL/MR/6180--98-8168, 1998.

4. "A User's Guide to FAST: Engineering Tools for Estimating Fire Growth and Smoke Transport", Richard D. Peacock, Paul A. Reneke, Walter W. Jones, Richard W. Bukowski and Glenn P. Forney, US Department of Commerce Special Report 921, 1997.

5. "Use of a Zone Model for Validation of a Horizontal Ceiling/Floor Vent Algorithm", J. L. Bailey, F.W. Williams and P. A. Tatem, NRL Memo Report 6811, 1991.

Appendix A

CFAST Keywords Used in Modeling of the Submarine Ventilation Doctrine Configuration

VERSN	Version of CFAST for which the input file is intended. A title may also be specified for identification purposes.
TIMES	Simulation time and frequency of on-screen and file outputs.
DUMPR	Name of output file to be used.
RESTR	Name of restart fire, if any.
FTIME	Event timeline.

Table A-1. Simulation Control Keywords

TAMB	Internal ambient temperature, pressure and reference elevation.
EAMB	External ambient temperature, pressure and reference elevation.

Table A-2. Ambient Environment Keywords

DEPTH	Depth (x-dimension) of the compartments, in meters. See FPOS.
WIDTH	Width (y-dimension) of the compartments, in meters. See FPOS.
HEIGH	Height (z-dimension) of the compartments, in meters. See FPOS.
HI/F	Floor elevation, relative to the reference elevation, in meters.
CEILI	Reference to an entry in the thermophysical properties database describing the ceilings.
WALLS	Reference to an entry in the thermophysical properties database describing the walls.
FLOOR	Reference to an entry in the thermophysical properties database describing the floors.
THRMF	Name of the thermophysical database to be used. If not specified, a default database, THERMAL.DF, is used.
HVENT	Definition of a horizontal vent, including the source and sink compartments, the vent number within the source compartment, the vent width and the heights of the soffit and sill.
VVENT	Definition of a vertical vent, including the source and sink compartments, the vent area and the shape (either round or square).
CVENT	Opening (width) of a horizontal vent as a fraction of the maximum width specified by the corresponding HVENT line.
CFCON	Enables vertical heat conduction through a ceiling to the floor of the compartment above.

Table A-3. Model Geometry Keywords

LFBO	Compartment number in which the main fire is located
FPOS	Coordinates (right-handed, Cartesian) of the fire location within the compartment relative to the lower, left, rear corner.
LFBT	Fire type. Type 1 is unconstrained by oxygen availability; type 2 is constrained.
FQDOT	Heat release rate of the burning fuel at the times specified by FTIME.
FMASS	Mass loss (pyrolysis) rate of the fuel at the times specified by FTIME
CHEMI	Miscellaneous parameters related to fuel combustion chemistry. Includes molecular weight and heat of combustion.
HCR	The mass ratio of hydrogen to carbon in the fuel.
O2	The mass ratio of available oxygen in the fuel to the total mass of fuel. This applies only to special cases, such as rocket fuels, in which the fuel consists of a mixture of oxidizing and reducing agents.
HC	Ratio of the mass of HCN produced by pyrolysis to the mass of fuel pyrolyzed.
HCL	Ratio of the mass of HCl produced by pyrolysis to the mass of fuel pyrolyzed.
CT	Ratio of the mass of a virtual "total toxics" product to the mass of fuel pyrolyzed. This product is taken to be representative of the combined toxic effects of the actual pyrolysis and combustion products.
OD	Mass ratio of soot to carbon dioxide in the combustion products. This parameter is very important for correct prediction of temperatures (reference [4]).
CO	Mass ratio of carbon monoxide to carbon dioxide in the combustion products.
FHIGH	Height of the base of the fire (above the reference position established by FPOS) at the times specified by FTIME.
FAREA	Horizontal area of the base of the fire at the times specified by FTIME.
CJET	Switches between the "standard" and "ceiling jet" model of convective heat transfer to the ceiling.

Table A-4. Fire Description Keywords